EXPERIMENTAL STUDY OF CALCIUM SULFATE (GYPSUM) CRYSTALLIZATION FROM STACK-GAS LIQUORS

by

David Lewis Etherton

A Thesis Submitted to the Faculty of the

DEPARTMENT OF CHEMICAL ENGINEERING

In Partial Fulfillment of the Requirements
For the Degree of

MASTER OF SCIENCE

In the Graduate College

THE UNIVERSITY OF ARIZONA

1 9 8 0

STATEMENT BY AUTHOR

This thesis has been submitted in partial fulfillment of requirements for an advanced degree at The University of Arizona and is deposited in the University Library to be made available to borrowers under rules of the Library.

Brief quotations from this thesis are allowable without special permission, provided that accurate acknowledgment of source is made. Requests for permission for extended quotation from or reproduction of this manuscript in whole or in part may be granted by the head of the major department or the Dean of the Graduate College when in his judgment the proposed use of the material is in the interests of scholarship. In all other instances, however, permission must be obtained from the author.

SIGNED: David Lewis Etherton

APPROVAL BY THESIS DIRECTOR

This thesis has been approved on the date shown below:

A. D. Randolph

A. D. RANDOLPH
Professor of Chemical Engineering

January 18, 1980
Date

But beyond this, my son, be warned:
the writing of many books is endless, and
excessive devotion to books is wearing to the body.

Ecclesiastes 12:12

ACKNOWLEDGMENTS

The author wishes to thank his advisor, Dr. Alan D. Randolph, for his guidance and encouragement throughout this project. Acknowledgment is also given to Dick VanReeth, in the College of Mines machine shop, and Frank Meyers, in the glass-blowing shop, for their excellent craftsmanship. A special thanks is given to the author's wife, Diane, for her patience while this work was being completed.

The author is indebted to the Electric Power Research Institute, Inc. (EPRI) for financial support under contract number RP1030-2. The following legal notice is required by EPRI.

This work was prepared by The University of Arizona as an account of work sponsored by EPRI. Neither EPRI, members of EPRI, nor The University of Arizona, nor any person acting on behalf of either:

a. Makes any warranty or representation, express or implied, with respect to the accuracy, completeness, or usefulness of the information contained in this report, or that the use of any information, apparatus, method, or process disclosed in this report may not infringe on privately owned rights.

b. Assumes any liabilities with respect to the use of, or for damages resulting from the use of, any information, apparatus, method, or process disclosed in this report.

TABLE OF CONTENTS

TABLE OF CONTENTS--Continued

LIST OF ILLUSTRATIONS

LIST OF ILLUSTRATIONS--Continued

LIST OF TABLES

ABSTRACT

The purpose of this study was to apply current crystallization technology to the crystallization of gypsum from stack-gas liquors, with the goal of increasing the product size. Growth and nucleation kinetics were determined in a "mini-nucleator" apparatus built for this study. The effects of pH level and chemical additives on nucleation rate, growth rate and crystal habit were also studied. The kinetic correlations obtained were used in the Mark I CSD simulator to predict the expected product size from various crystallizer designs.

Gypsum was shown to nucleate by secondary nucleation mechanisms when large (> 150 microns) crystals were retained in the crystallizer. However, bursts of primary nucleation occurred if the supersaturation was too high, too few seeds were present or the pH was suddenly reduced. Bursts of primary nucleation would significantly reduce the product size. Citric acid was found to be an effective habit modifier, forming blockier crystals which would be easier to filter. The results of the CSD simulations showed that by using a double-drawoff crystallizer the product size can be nearly doubled which would greatly improve the ease of disposal.

CHAPTER 1

INTRODUCTION

Development of effective and reliable methods for removal of SO_2 from stack gases of coal-fired plants is important to the nation's energy future. This task looms especially important in light of recent mandates to reduce reliance on imported oil by shifting to coal-fired plants. Many flue gas desulfurization (FGD) processes have been developed over the last 20 years and several processes are successfully being used in full-scale operation.

The most common commercial process is the lime/limestone scrubber. In this process, SO_2 is absorbed by a slurry of lime or limestone which reacts to form calcium sulfite or, if excess air is supplied, calcium sulfate. The sulfite-sulfate is precipitated as a fine solid and is disposed of as land fill. Figure 1 shows a typical scrubber configuration.

One of the problems of this process is that the solids produced are relatively small, requiring large clarifiers and filters to dewater the sludge enough to make an acceptable land-fill. The purpose of this study was to determine fundamental crystallization kinetics of calcium sulfate dihydrate (gypsum) systems and to use these kinetic expressions in a crystallizer simulation to indicate how crystallizer design might

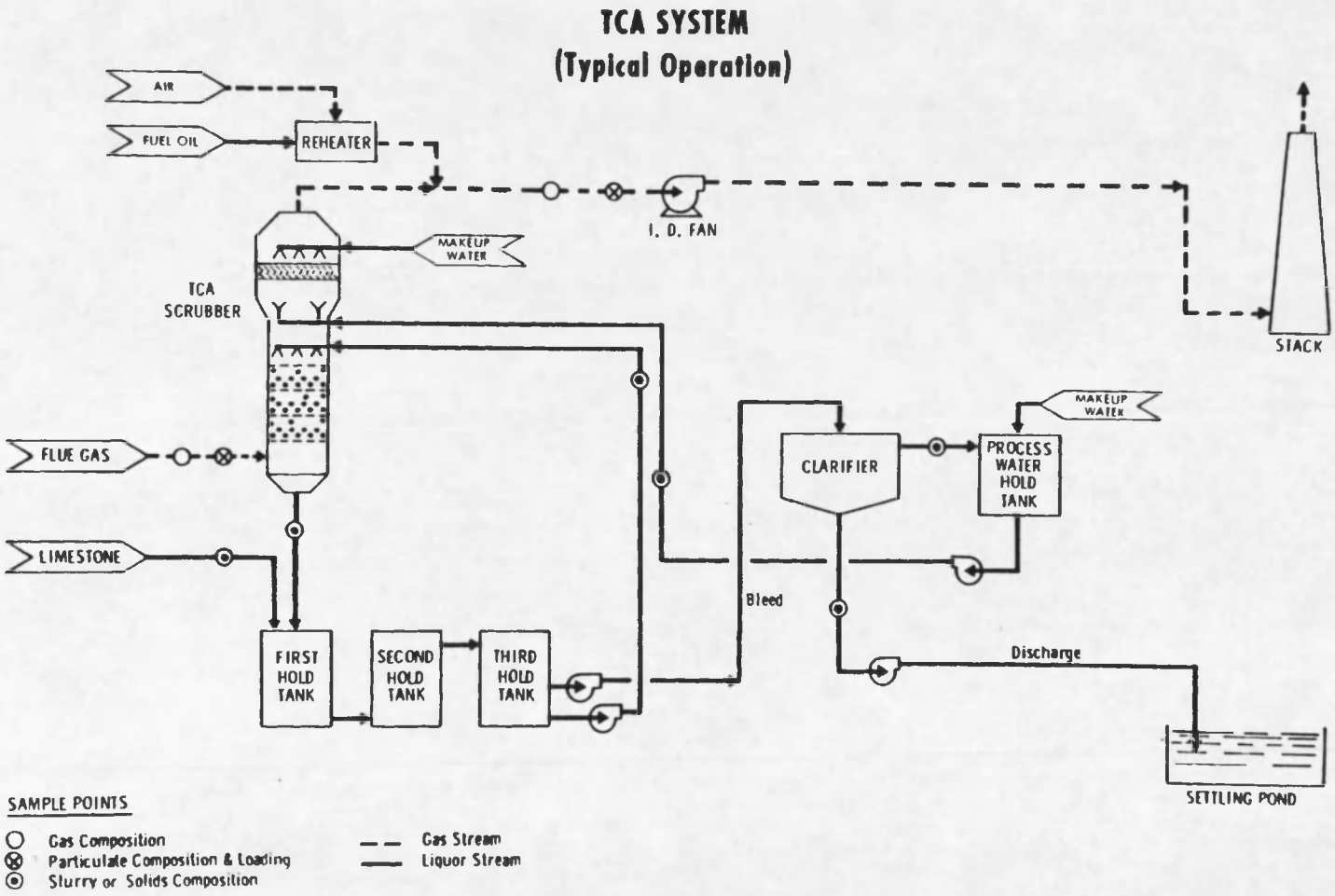

Figure 1. Flow Diagram of Typical Scrubber.

be used to improve product size, thus producing a waste sludge having better landfill characteristics.

The kinetic experiments were carried out in a 1-liter, well-mixed crystallizer. Supersatuation was created by adding K_2SO_4 solution to a simulated stack-gas liquor solution containing calcium, magnesium, sodium, chloride, and sulfate ions. Seed crystals were added and retained in the crystallizer by a 150 micron screen. The secondary nuclei produced were passed through the screen to a Particle Data, Inc., particle counter where the size and number of particles were determined. These data were analyzed by an adjoining mini-computer.

A previously developed crystallization simulation program (the Mark I simulator) was used to model various crystallizer configurations. This progran can be used to predict the effect on product size of changes in liquid vs. solid residence time and change in solids residence time as a function of size.

The main approach of this study was thus to measure gypsum crystallization parameters (growth and nucleation rate) as a function of process conditions and chemical environment, to correlate these data in useful empirical kinetics expressions and to make predictions of how particle size could be increased with changes in the process environment and/or precipitator configuration.

CHAPTER 2

EXPERIMENTAL APPARATUS

This section describes the experimental equipment used to study the crystallization of calcium sulfate from simulated stack-gas liquors. Also discussed are the reasons for the selection of an open-loop system instead of a closed-loop system.

Apparatus Development

The "mini-nucleator," as developed at The University of Arizona, is a closed-loop system. Liquid leaving the crystallizer passes through a saturator packed with the material being crystallized and then back to the crystallizer. Supersaturation is attained by operating the crystallizer at a lower temperature than the saturator. This configuration works well for materials that have high solubilities that are temperature dependent.

Since $CaCO_4$ has a low solubility which varies only slightly with temperature, supersaturation was attained by chemical reaction in the crystallizer. In this case, the saturator would act as a desupersaturator, that is, any supersaturation that was not relieved in the crystallizer should be relieved in the saturator. It was discovered that this was not happening, due to the combination of low growth rates and low residence times (ca. 15 min). Therefore, all of the supersaturation was not relieved and the concentration would continue to rise

to unknown values until bursts of homogeneous nucleation would relieve the system and the concentration build-up would start again.

Because of this problem, an open-loop system was implemented. In an open system, the liquid leaving the crystallizer was discarded rather than being recycled. The advantage of this is that the supersaturation can be set by the level of feed concentration. The open-loop configuration proved advantageous when studying the effects of additives and pH level, as foreign ions would not build up in the system. The open system did have the drawback of requiring a new solution for each run. This drawback, however, was not serious due to the small volume of the crystallizer and the inexpensive feed chemicals.

Apparatus Description

The experimental apparatus consists of a feed tank, flow measurement cylinder, feed pump, pre-heater, filter array, crystallizer, counter cell, level control, additive pumps, stirrer, temperature control bath, and the Particle Data, Inc., particle counter with PDP-8 mini-computer and dewriter attachments. Figure 2 is a schematic of the apparatus showing the flows of materials and information.

The liquor feed tank was a 20-liter Nalgene aspirator bottle with a valve at the bottom. Liquor flowed from the tank through a 250-ml graduated cylinder. By closing the valve from the tank, the flow rate could be measured by timing the flow out of the cylinder. The liquor was pumped from the cylinder using a M-Roy^{R} variable flow diaphragm pump.

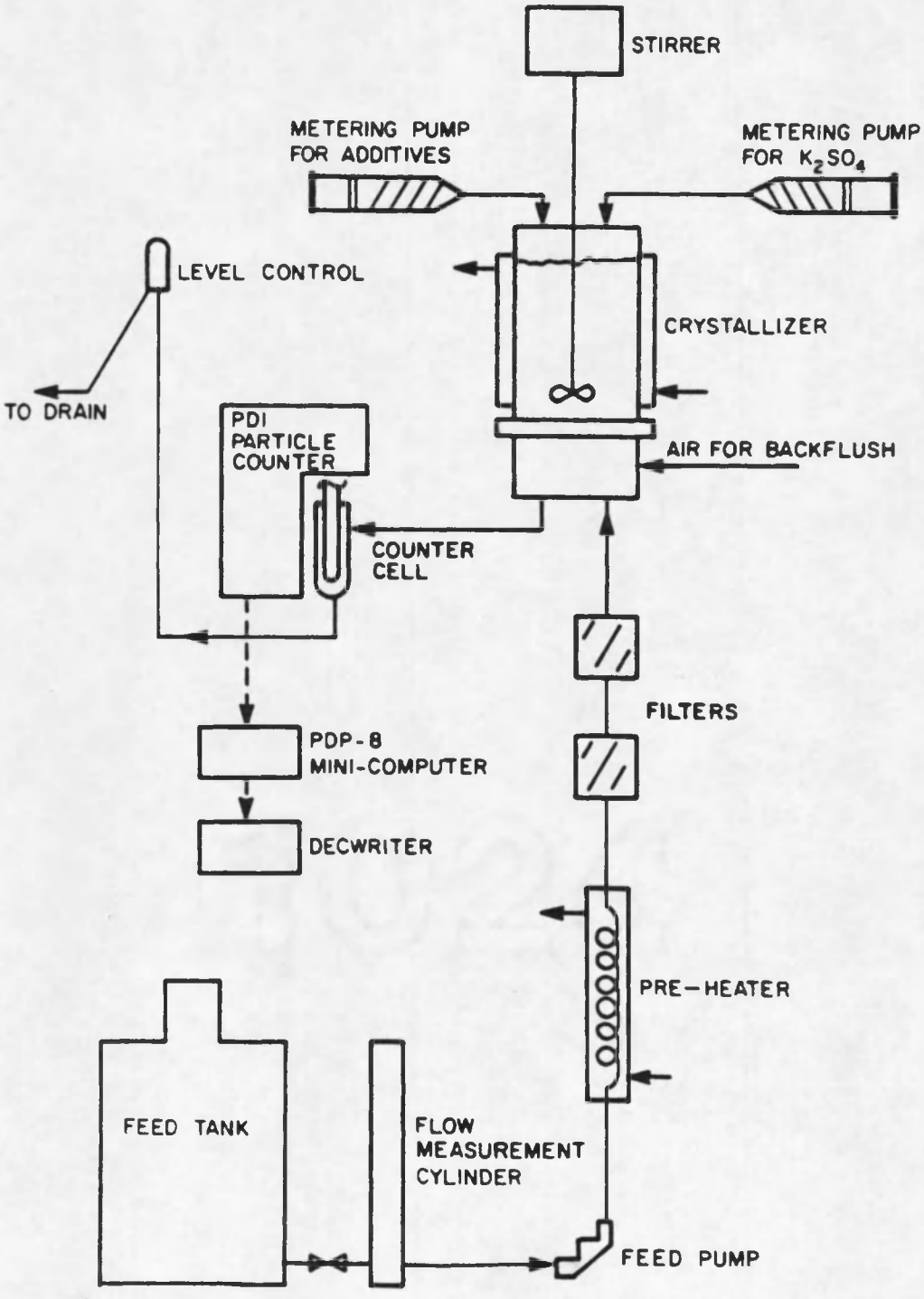

Figure 2. Schematic of Experimental Apparatus.

The preheater was a 12-inch glass condenser tube. The temperature of the preheater was kept the same as the crystallizer. Its purpose was to heat the liquor to near operating temperature. Following the preheater were two Pall^{R} micropore filters. The first filtered to 3.0 microns and the second filtered to 0.2 microns. The purpose of the filters was to insure that a particle-free liquor entered the crystallizer.

The crystallizer was a one-liter, jacketed glass vessle which was built by the University of Arizona Glass Shop (Figure 3). On top of the vessel were 5 standard taper joints which were used for seed and additive introduction, a thermometer, and the stirrer shaft. The bottom was flared and ground so as to seal to the base plate.

The base plate was machined from Plexiglas^{R} and was clamped to the crystallizer by three Plexiglas^{R} clamps. The base plate was fitted with one feed port and two drawdown ports, one screened and one unscreened, and a hydraulic flush port. The screened port was a conical-shaped opening covered by a 100-mesh stainless steel screen. The screen caused the seed crystals to be retained in the crystallizer but allowed the nuclei to pass to the counter. A rubber diaphragm was placed over a back-flush to prevent the screen from plugging. The unscreen port was used to drain the crystallizer after a run.

A draft tube baffle was supported inside the crystallizer by four Teflon^{R} wedges. The baffle was sized to give equal flow area in the center and annulus. The action of the impeller causes fluid to flow

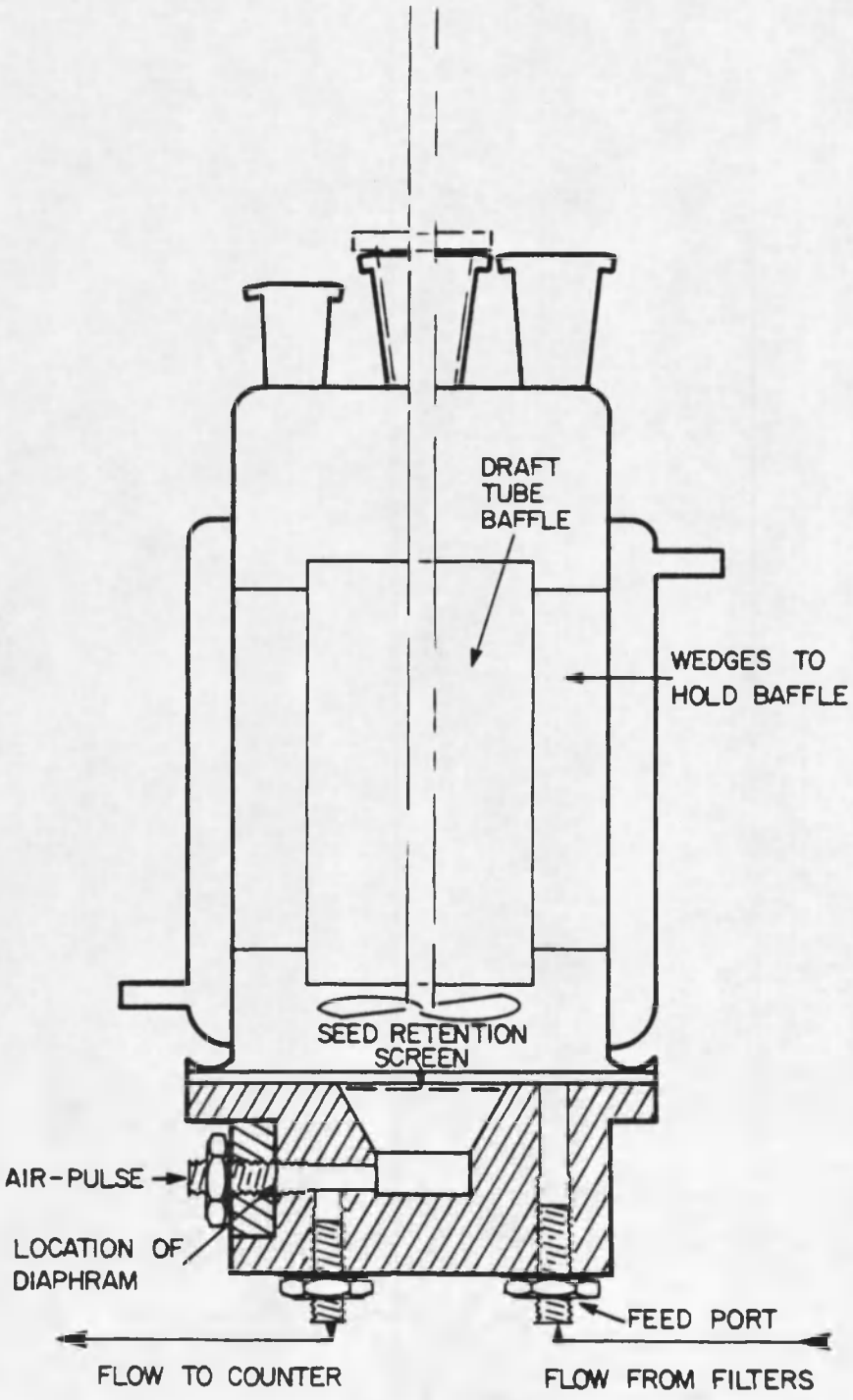

Figure 3. Crystallizer and Base Plate.

down the middle and up the outside. Thus, the seed crystals are well-suspended in the liquor.

The liquor flowed from the crystallizer to the counting cell of the Particle Data counter through the level control and to the drain.

The stirrer was of variable speed drive manufactured by Bench Scale Equipment Co. A stainless steel shaft entered the crystallizer through the center T-S joint with a machined Plexiglas^{R} bushing. The impeller was a four-blade propeller type two inches in diameter. ISCO model 312 metering pumps were used to pump K_2SO_4 reactant and the additives into the crystallizer. A Haake model FE temperature controller bath was used to heat both the crystallizer and the preheater.

The Particle Data, Inc. (PDI), particle counter uses the zone sensing principle to determine the number and size of particles. The sensing mechanism consists of an orifice with an electrode on each side. An electrolyte solution with particles suspended in it is drawn through the orifice by a vacuum pump. As a particle passes through the orifice, the resistivity of the solution is changed. The change in resistivity is proportional to the volume of the particle. The particle size is converted to a logarithmic scale and the number of particles as a function of size is shown on an oscilloscope. The PDP-8 mini-computer converts the data to population density and calculates the CSD parameters. The output is printed on a DEC-writer terminal. Figure 4 shows a typical output.

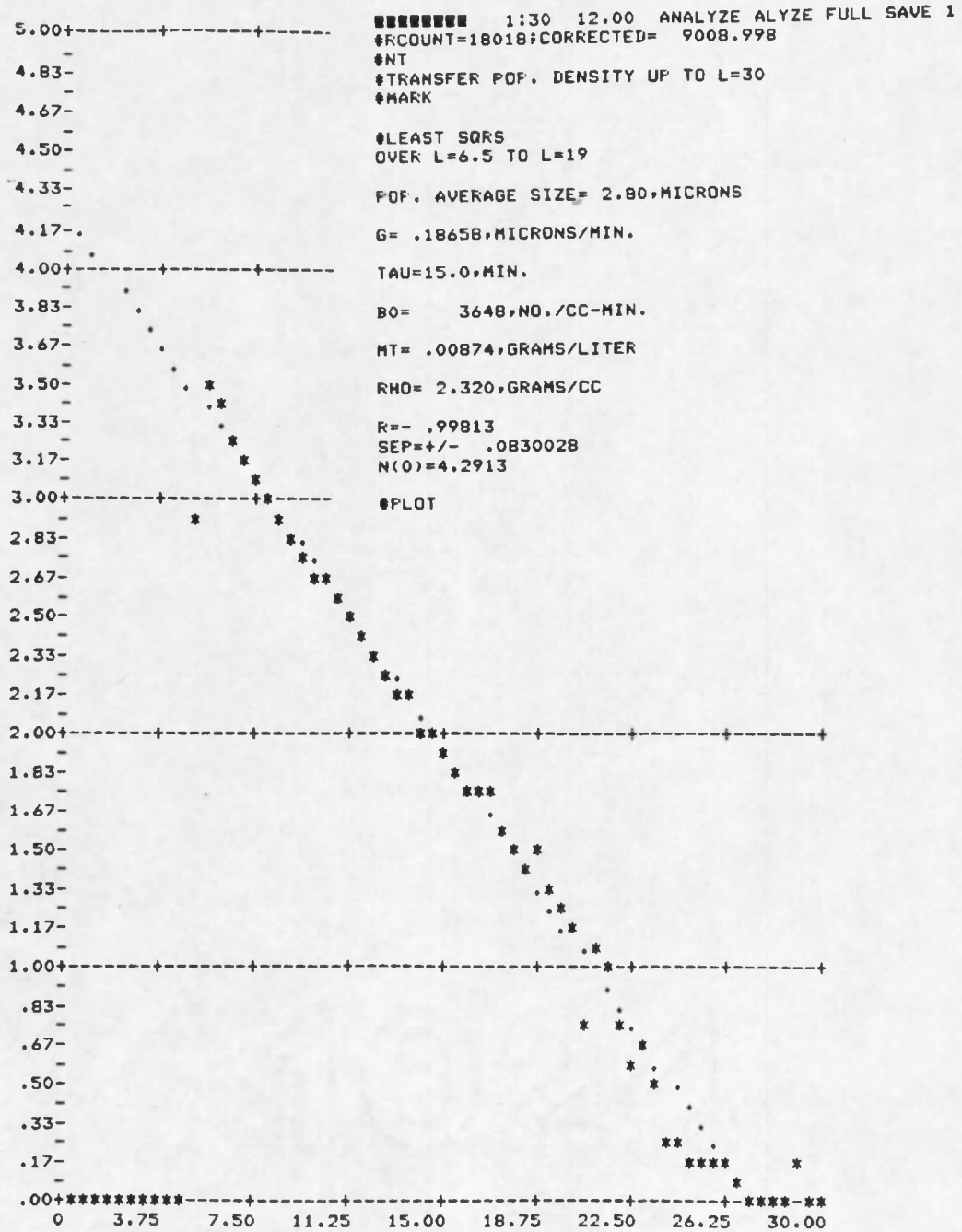

Figure 4. Typical Output from PDI Counter.

CHAPTER 3

EXPERIMENTAL PROCEDURES

This section describes the general procedures used during this study. It covers the calibration of the apparatus, the make-up of solutions, the growth of seed crystals and a description of a typical run. Those procedures that are unique to a particular part of the study are discussed in the relevant section describing that run.

Calibrations

The following calibrations were performed initially and/or periodically through the course of the study: crystallizer volume, liquor feed pump, reactant and additive pump rates, pH meter, stirrer speed, and particle counter.

The crystallizer volume was calibrated by adding 1.25 liters water and marking the level. Water was then drained out in 0.05-liter increments and each level marked. The volume of the cone under the screen was full throughout the process.

The liquor feed rate was measured by filling the flow measurement cylinder and closing the valve from the feed tank. A flow of 100 ml was timed and the flow rate calculated. The reactant and additive pumps were calibrated in the same manner. These flow measurements were made at the beginning of each run and several times during the run.

The pH meter was calibrated using two buffers, one of pH 4.0 and the other of pH 7.0, as per the instructions supplied with the instrument. Recalibration was performed once a week. The stirrer RPM was calibrated roughly using a mechanical tachometer and then fine-tuned with an electronic stroboscope. The RPM was checked at the beginning of each run.

The particle counter was calibrated using particles of a known mean size and a narrow size distribution, in this case ragweed pollen. This material has a uniform size of 19.5 microns. By adjusting the current and gain controls of the counter, the peak of the size distribution can be made to appear in different channels. The location of two of the peaks is input to the mini-computer as the calibration points. The calibration of the counter was checked several times during the study and was found to be quite stable.

Solution Make-Up

The solutions needed for each run were the feed liquor and the K_2SO_4 reactant. The feed liquor had the following concentrations of ions: calcium -- 1.79 g/L; magnesium -- 0.20 g/L; sodium -- 0.05 g/L; sulfate -- 1.79 g/L; and chloride -- 2.51 g/L and was made up with the following salts: calcium sulfate dihydrate -- 1.80 g/L; calcium chloride -- 3.80 g/L; magnesium sulfate -- 0.99 g/L; and sodium chloride -- 0.13 g/L. To make the feed liquor 72.0 g of calcium sulfate were placed in the 40-liter make-up tank and about 38 liters of water were added. This mixture was stirred overnight to dissolve all the calcium sulfate. In the morning, the remaining ingredients were added.

The K_2SO_4 reactant was made by adding 69.6 g of K_2SO_4 to a one-liter volumetric flask and filling to the mark with water. This gave a solution with a molar concentration of 0.4.

The actual stack-gas liquor supplied by the Shawnee facility was used in only two runs. Since the concentrations of ions in this liquor were not known, the calculation of supersaturation was impossible. For the two runs that were made (noted in Appendix B), the supersaturation was not accurately known. However, the results were within the range of the data from the synthetic liquor.

Preparation of Seed Crystals

It was discovered that seed crystals were required to stimulate crystallization in a reproducible manner. Therefore, it was necessary to have a supply of seed crystals with regular shapes in the size range 175-300 microns. Initially, seed was produced by mixing concentrated solutions of calcium chloride and sulfuric acid together. The nuclei that were formed by this reaction were then grown to the appropriate size. The crystals were grown by retaining the nuclei in the crystallizer and flowing a supersaturated solution of calcium sulfate through the crystallizer until the crystals were as large as needed. The seed produced in this manner were quire irregular in shape (Figure 5a) and therefore were not suitable.

It was discovered that the calcium sulfate powder that was being used for feed liquor make-up contained some single crystlas that had not

a)

b)

Figure 5. Seed Crystals: a) Initial Attempts; b) Seeds Used.

been pulverized in the manufacturing process. These crystals were separated by sieving and grown in the same manner as above. After growth, the crystals retained their shape (Figure 5b) and were therefore suitable for use as seed. After enough seed was grown, they were sieved into narrow size distributions and stored for use as needed.

Typical Run

The procedures involved in making a run were standardized and followed the basic format of run preparation, initiation, data collection and termination. At the start of a run, the feed liquor was transferred to the feed tank and the pump was turned on at the maximum flow rate while the liquor was pumped through to purge the system. Calgon^{R} detergent, which is used to prevent fouling, was then drained from the crystallizer which was rinsed with water several times. The liquor flow rate was adjusted to approximately the correct value and the crystallizer allowed to fill. The K_2SO_4 feed pump, air pulse and the stirrer were also turned on and adjusted at this time. The temperature bath was operated continuously to minimize heat-up time. While the crystallizer was filling, the particle counter and the mini-computer were turned on and the counter cell was flushed out. As the level approach the one-liter mark, the level control was adjusted to maintain that level. The seeds were added about 30 minutes after the crystallizer was filled. This represents time "zero" for data analysis purposes.

A 15-minute to 2-hour induction time was observed before nucleation began to occur and/or the crystals grew to measurable size. The steady-state population distribution was reached within an hour after

nuclei crystals were observed. The initiation of nucleation and attainment of steady state was observed using the particle counter. Since the particle counter is "on-line," the crystal size distribution in the crystallizer can be monitored continuously and is known at any time during a run. The PDP-8 mini-computer performed an analysis of CSD as outlined in Chapter 1 and outputted the crystallization parameters and a plot of the population density to the DEC-writer. These data were then available for later analysis. When a sufficient amount of data has been taken the run was stopped.

At the end of the run, the entire contents of the crystallizer was drained through the unscreened drawdown port. The seed crystals were filtered, dried and weighed and then placed in sample bottles for future analysis (i.e., photographs to observe crystal habit). The entire flow system, including reactant and additive pumps, was flushed with water to prevent fouling in case the liquors evaporated. A dilute Calgon^{R} solution was left in the crystallizer. All systems except the temperature bath were shut off.

CHAPTER 4

LITERATURE AND THEORY

Crystallization involves the creation and growth of a solid phase from solution. Since the crystallization process creates new entities, mass and energy balances are not sufficient to describe the process. Therefore, a population balance is needed to account for particles entering and leaving the system. By using the population balance to analyze the product from a crystallizer, the nucleation rate and growth rate can be determined from measurements of the crystal size distribution. The nucleation and growth rates can then be correlated with the pertinent variables to give a design-useful kinetic correlation.

Population Balance

The population balance is given by Randolph and Larson (12) as:

$$\frac{\partial n}{\partial t} + \frac{\partial (Gn)}{\partial L} + n \frac{\partial (\ln V)}{\partial t} = - \sum_i \frac{n_i \bar{Q}_i}{V} + B(L) - D(L) \qquad [1]$$

For the ideal MSMPR crystallizer (i.e., steady state, no crystal breakage, perfect mixing, and no crystals in the feed), this equation becomes:

$$\frac{d(Gn)}{dL} = - \frac{n}{\tau} \qquad [2]$$

which predicts a population density distribution of the form:

$$n(L) = \frac{B^{o}}{G} \exp\left(\frac{-L}{G\tau}\right) \qquad [3]$$

where n(L) = population density (number/micron·cc);

G = linear growth rate (micron/min);

B^{o} = nucleation rate (number/cc·min);

L = linear particle size (micron); and

τ = residence time (min).

This equation predicts that a plot of $\log_e$ n(L) vs. L gives a straight line with a slope of $-1/G\tau$ and an intercept of B^{o}/G.

Nucleation

Nucleation is the formation of new crystals of a solute from a supersaturated solution. Three types of nucleation are:

1. Homogeneous nucleation -- the appearance of new crystals as a result only of supersaturation.
2. Heterogeneous nucleation -- the appearance of new crystals in the presence of foreign substrates.
3. Secondary nucleation -- the appearance of new crystals in the presence of seed crystals of the same material.

The rate of homogeneous nucleation is given by an Arrhenius rate expression:

$$B^{o} = C \exp(\Delta G^{*}/kT) \qquad [4]$$

Heterogeneous nucleation rate is given by a similar equation but with a term to account for the lowering of the energy barrier in the presence of impurities which act as nucleation sites. Both homogeneous and heterogeneous nucleation exhibit a metastable limit of supersaturation below which nucleation will not occur. This limit occurs at a relatively high supersaturation, much higher than in an industrial crystallizer. Therefore, it is likely that some other mechanism is responsible for nucleation in these cases.

Clontz and McCabe (3) showed that nuclei can be formed at supersaturations below the metastable limit by lightly tapping a crystal in solution. There was no visible damage to the crystal. It was therefore proposed that nuclei were formed by dislodging part of a growth layer surrounding the crystal. In an industrial crystallizer, secondary nucleation can be a result of crystal-crystal, crystal-impeller or crystal-wall contacts. Secondary nucleation has been shown to be proportional to the supersaturation and the intensity and frequency of the collisions (2, 5, 13).

A common form for the correlation of nucleation rate data is:

$$B^{\circ} = k_N(\text{RPM})\ G^i M_T^j \qquad [5]$$

The growth rate (G) is proportional to supersaturation but is more easily measured. The slurry density (M_T) is a measure of the amount of crystals present (related to the collision frequency) and the RPM is related to collision intensity. This power-law type of correlation has

been used with much success by many investigators to correlate secondary nucleation data (8, 11, 15).

Growth

Crystal growth is a mass transfer operation where solute molecules in solution become part of a solid crystal. Supersaturation is the driving force necessary for crystal growth. For growth to occur, the solute must diffuse to the crystal surface and then become integrated into the crystal lattice. Growth can, therefore, be diffusion-rate controlled or integration-rate controlled. With low mixing intensity, growth is generally diffusion-controlled but is integration-controlled with high mixing. The accepted mechanism of solute integration is the screw-dislocation theory presented by Burton, Cabrera and Frank (1). According to this mechanism, solute is added to the crystal at imperfections in the crystal lattice. The imperfection is continued in a spiral direction, thereby perpetuating its existence.

Theoretical considerations predict growth as a function of supersaturation (S) as either

$$G = k_G S \qquad [6]$$

or

$$G = k_G S^2 \qquad [7]$$

However, in order to achieve a better fit of experimental data, a power-law model of the form

$$G = k_G S^a \qquad [8]$$

is normally used. This power law is the form used to correlate the data in this study.

CHAPTER 5

RETAINED SEED

Experiments with retained seed dealt both with the effects of the seeds on the crystallization parameters and the effect of other variables on the seeds. Nucleation rate is affected by the size and number of seed crystals and also the seed growth rate. Nucleation rate is correlated with these variables to give a kinetic expression. The seed exhibit a growth rate and crystal habit characteristic of the conditions present. Growth rate is correlated with supersaturation to give a kinetic expression. The crystal habit is affected by the growth rate and by agglomeration. SEM micrographs are used to show the variations in habit.

Growth Rate

Seed Growth Rates

Seed growth rates are needed for both the correlation of growth vs. supersaturation and for determining the effect of growth rate (supersaturation driving force) on B^{o} as discussed in Chapter 4. The seed growth rates used in this study were calculated using Equation 9:

$$G_s = \frac{L_f - L_i}{\Delta t} \qquad [9]$$

The final size (L_f) was calculated from Equation 12, which was derived from Equation 10:

$$m = \rho k_v L^3 \qquad [10]$$

where m = mass of seed crystals;

ρ = crystal density;

k_v = shape factor; and

L = characteristic crystal length.

Equation 10 gives the relationship between the size and the mass of crystals having similar shapes. Writing this equation for the beginning and end of a run gives:

$$\left(\frac{m}{L^3}\right)_i = \left(\frac{m}{L^3}\right)_f \qquad [11]$$

or by rearranging:

$$L_{final} = \left(\frac{m_i}{m_f} L_i^3\right)^{1/3} \qquad [12]$$

The initial size was taken as the geometric mean of the sieved seed fractions and the mass of the seeds was measured before and after a run. The data and calculated results are given in Appendix A.

Growth vs. Supersaturation Correlation

Crystal growth rate is dependent on the supersaturation driving force, and therefore a correlation of growth rate vs. supersaturation is necessary to compute CSD and yield from a scrubber system. In two

component non-ionic systems (i.e., solute and solvent), solubilities are readily defined; however, in multi-component ionic systems (such as stack-gas liquor), the solubility is interdependent on the ionic equilibria of the solution. A computer routine called the Bechtel Modified Radian Equilibrium Program (BMREP) has previously been developed by Radian Corp., and Bechtel Corp., which calculates all the solution equilibria for the components commonly found in stack-gas liquors. This program requires as inputs the ionic concentrations that are fed to the crystallizer and calculates equilibrium concentrations. The value given for the equilibrium solids concentration is taken as the feed supersaturation of crystallizable solute, i.e., gypsum in this case.

This value is not the actual supersaturation driving force existing in the crystallizer because some of this material has been precipitated by growth on the seed and created nuclei. The amount grown on the seed can be converted to grams/liter (the units of supersaturation) by dividing the mass gain by the run time and the liquor flow rate. It was found that such growth accounted for 10-40% of the supersaturation. The mass of the nuclei was calculated by the mini-computer from the measured fines size distribution. The mass of the nuclei was found to account for 0.5 to 3% of the feed supersaturation. Since this was small compared to the seed growth and because the mass of the nuclei tended to fluctuate during a run, it was not subtracted from the feed supersaturation. The actual supersaturation in the crystallizer was given by the equilibrium solids calculated from the BMREP minus the

supersaturation relieved due to seed growth. The data and results of these calculations are also given in Appendix A.

A growth rate vs. supersaturation correlation was obtained in the form of a power-law model using a library multiple linear regression computer routine. Thus:

$$G_s = \exp(13.11)\ S^{2.226} \quad ; R^2 = .952 \qquad [13]$$

The units of S are g/cc here since those are the units used by the Mark I CSD simulator to be used in subsequent calculations. The data used for this correlation and the correlation line are shown in Figure 6.

Crystal Habit

The habit of the seed crystals can be affected both by high growth rates and by agglomeration at high concentrations of fine crystals. Figure 7 is the growth correlation plot showing several points that have higher than expected growth rates. From SEM micrographs of the seeds (Figure 8), it can be seen that the seeds having higher than expected growth rates are agglomerated with the fine crystals much more than the seeds having growth rates that are in line with the correlation.

The growth rate also affects the crystal habit. Figure 9 shows seeds having high and low growth rates. The seeds with higher growth rates exhibit more random growth and also some agglomeration when compared to low growth seeds.

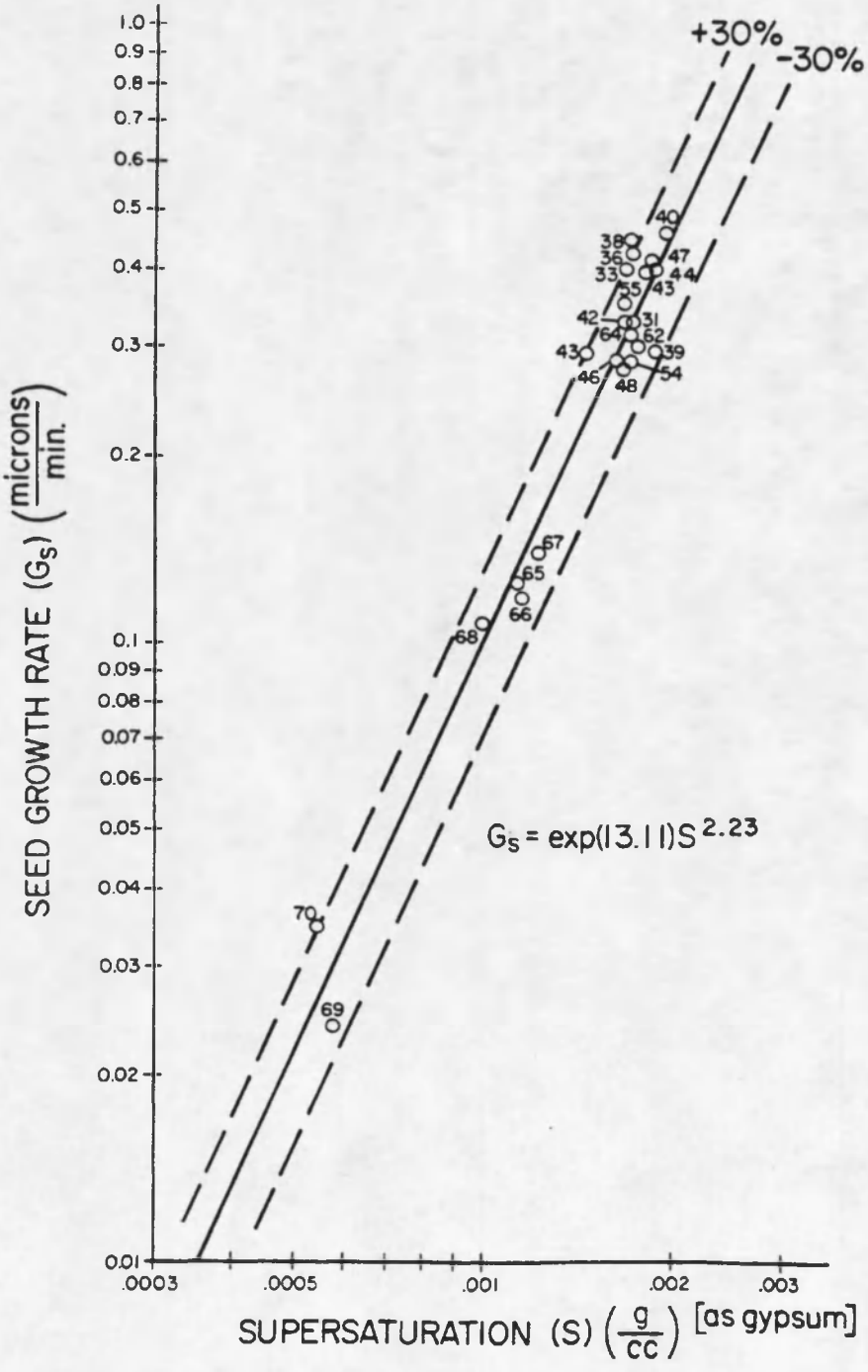

Figure 6. Growth Rate Correlation.

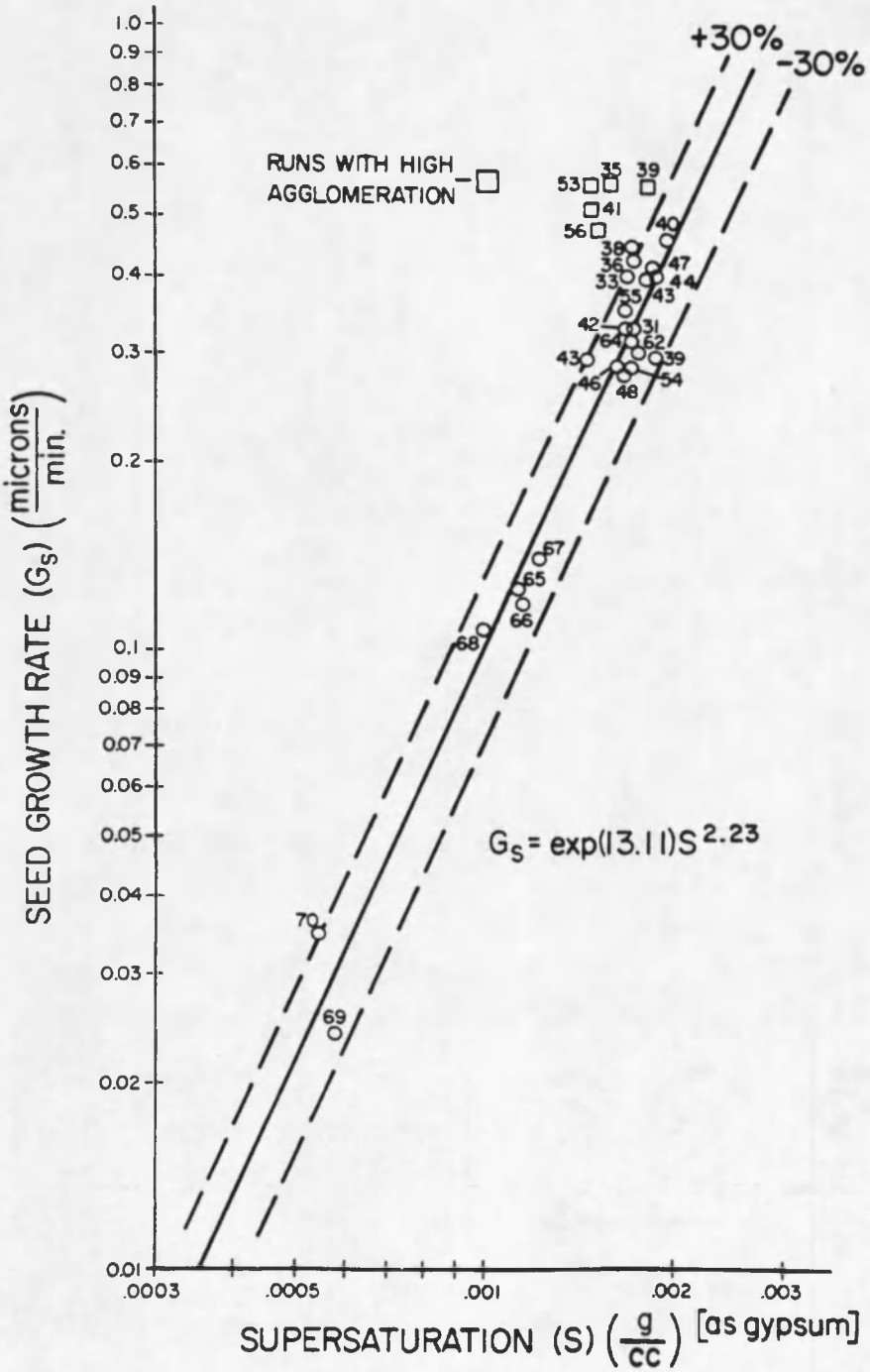

Figure 7. Growth Correlation Showing Points with High Agglomeration.

a)

b)

Figure 8. Seed Crystals: a) From Run #35 Showing Agglomeration with Fines; b) From Run #36 Showing Less Agglomeration.

a)

b)

Figure 9. Seed Crystals: a) From Run #45 (High Growth Rate); b) From Run #48 (Low Growth Rate).

Nucleation

Primary vs. Secondary Nucleation

In order to determine the relative importance of primary vs. secondary nucleation, several runs were made with and without retained seeds. The data from these runs are shown in Table 1. The major conclusion reached here is that the use of retained seed causes reproducible sustained nucleation; without retained seed, the occurrence of nucleation is not reproducible. Because of these results, all further runs were made with retained seed. The data obtained were analyzed by assuming a secondary nucleation mechanism. Further information on secondary nucleation is provided by study of the effects of growth rate and seed mass on nucleation rate.

Table 1. Effect of Parent Seed on Sustained Nucleation.

Run #	Feed Supersaturation (g/L)	Seed	Comments
13	1.95	not retained	no nucleation
14	2.13	retained seed	nucleation sustained
16	2.13	retained seed	nucleation sustained
17	2.13	not retained	nucleation sustained
18	1.95	not retained	no nucleation
19	2.13	not retained	no nucleation
20	2.13	retained seed	nucleation sustained

Effect of Growth Rate and Seed Mass on Nucleation Rate

As discussed in Chapter 4, the growth rate and the amount of seed are two of the parameters affecting nucleation rate. The usual way to model this dependence is by a power law of the form:

$$B^o = k_N G^i M_T^j \qquad [14]$$

G can be changed experimentally by varying the supersaturation. M_T can be varied by changing either supersaturation or the initial weight of seed added. Since the seed crystals are completely retained during a run, their mass will depend on the growth rate. Therefore, increasing the supersaturation will also increase M_T. If M_T is increased by adding more seed, then the supersaturation will decrease due to the extra solute depleted by more seeds. The overall effect of the interdependence is stabilizing due to the inverse relation of S on M_T.

Because of this interdependence, it is difficult to vary G at constant M_T or vary M_T at constant G. Therefore, it is necessary to separate the dependence of nucleation rate on M_T and G by multiple variable curve fitting. The data for 28 runs (from Appendix B) were fit by a multiple linear regression routine to give the B^o correlation. Thus:

$$B^o = \exp(16.72)\ G_s^{1.48}\ M_T^{1.27} \qquad [15]$$

having an R^2 value of 0.83. These data are plotted as $B^o/M_T^{1.27}$ vs. G in Figure 10. Also shown is the correlation line and the 30 and 30% error

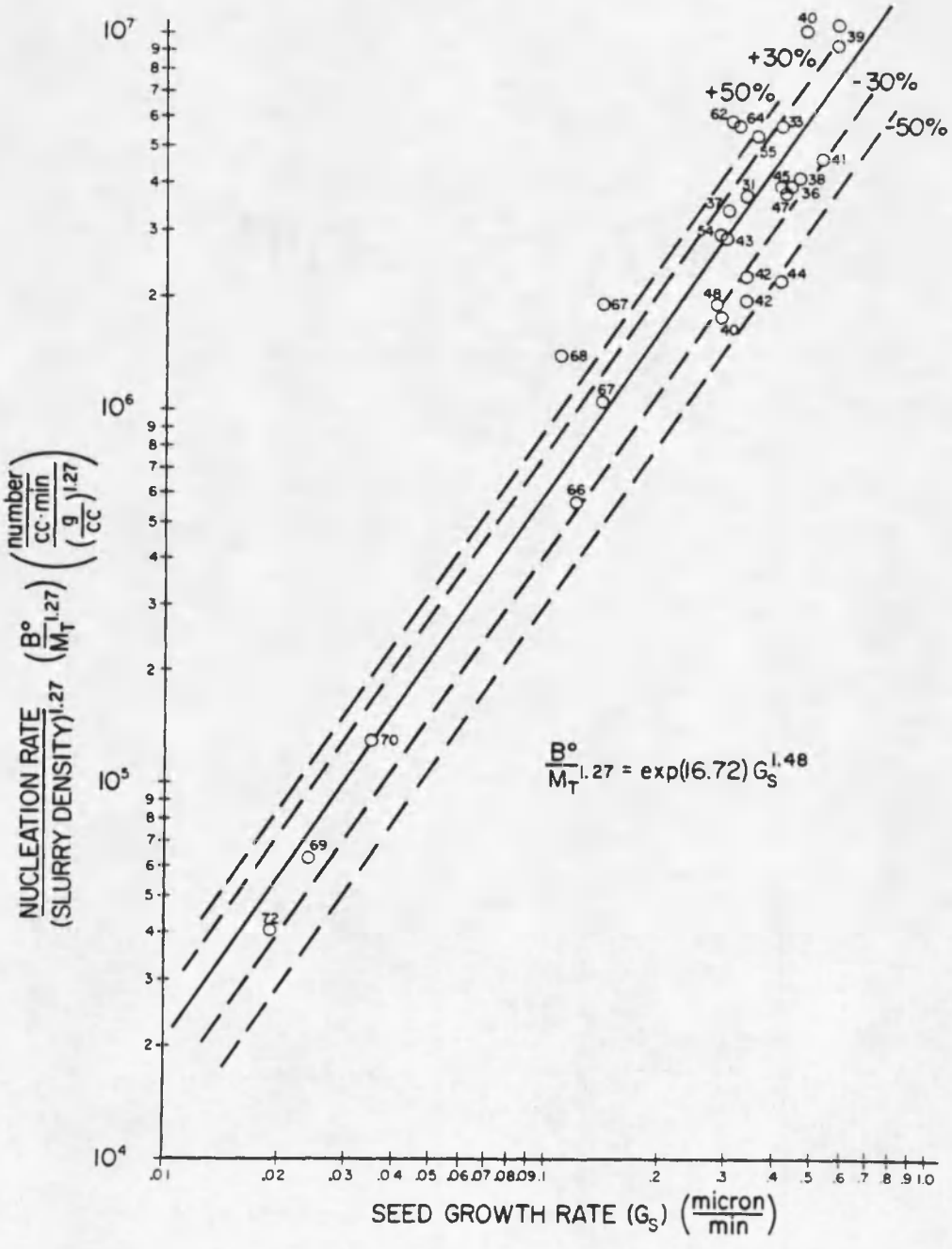

Figure 10. Nucleation Rate Correlation.

limits. Figure 11 is a plot of experimental nucleation rate vs. the nucleation rate calculated by the correlation.

RPM Changes

As stated in Chapter 4, the stirrer speed is also a variable which affects the rate of secondary nucleation. Most of the runs in this study were performed at a constant RPM. However, during the several runs in which the RPM was changed during the run, a change in nucleation was observed (Table 2).

The fact that nucleation rate increases with increasing RPM is another indication that nucleation is occurring by secondary mechanisms.

Comparison with Other Data

Ottmers et al. (10) have studied precipitation rate (nucleation plus growth) of calcium sulfate on a bench scale. In their experiments, the crystallizer was seeded with about 5 g/liter of 100 micron seeds. Both the seed and the nuclei were retained in the crystallizer until the end of the run. The precipitation rate was determined by the difference between inlet and outlet solution concentrations.

They found that at supersaturation ratios below 1.3 to 1.4 only growth occurred and above that level nucleation started to occur. The presence of nucleation was inferred by the rapid increase in precipitation rate (see Figure 12) and by the visual observation of many fine crystals in the crystallizer. They also found that stirrer speed had no effect on the precipitation rate. A kinetic expression, relating the

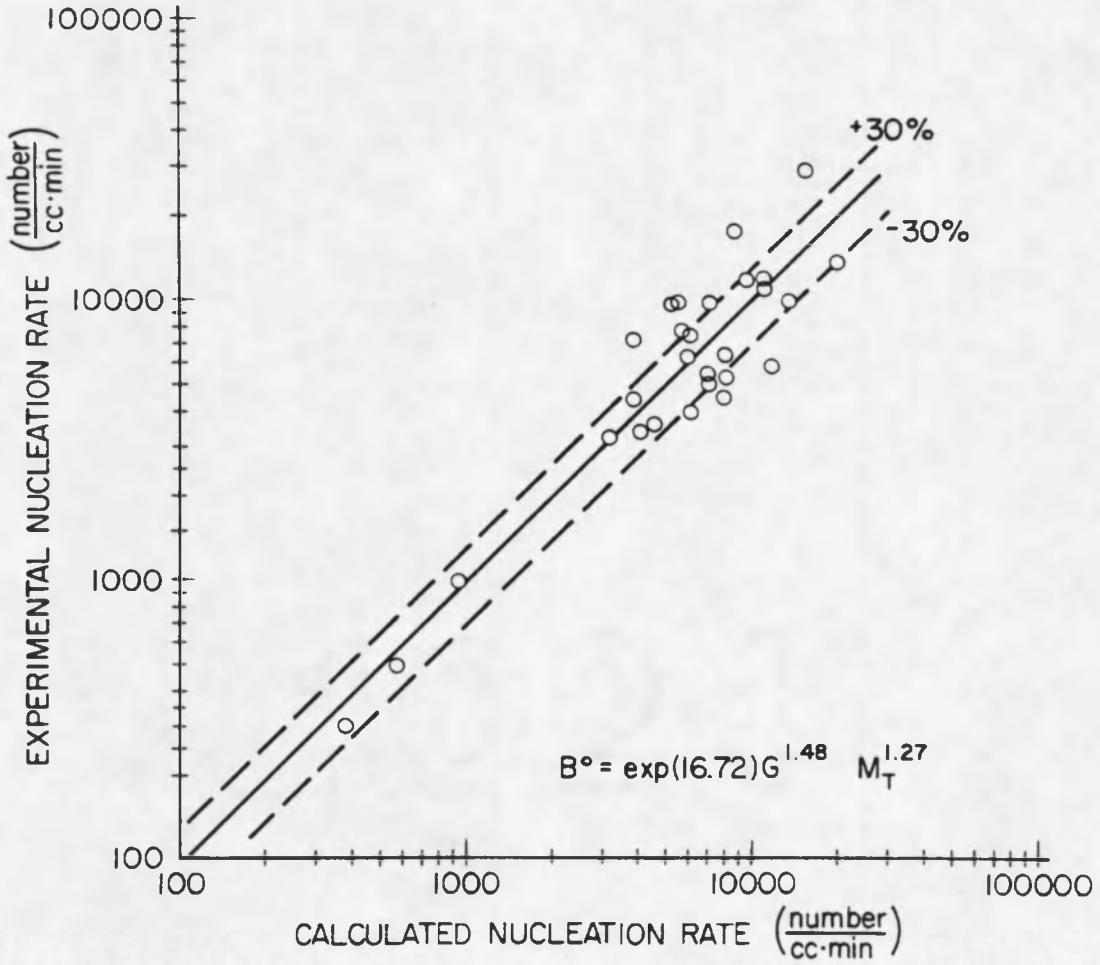

Figure 11. Experimental vs. Calculated Nucleation Rate.

Table 2. Effect of RPM on Nucleation Rate.

Run #	RPM	B^{o}	RPM	B^{o}
31	300	3700	450	6400
48	300	3500	450	5100

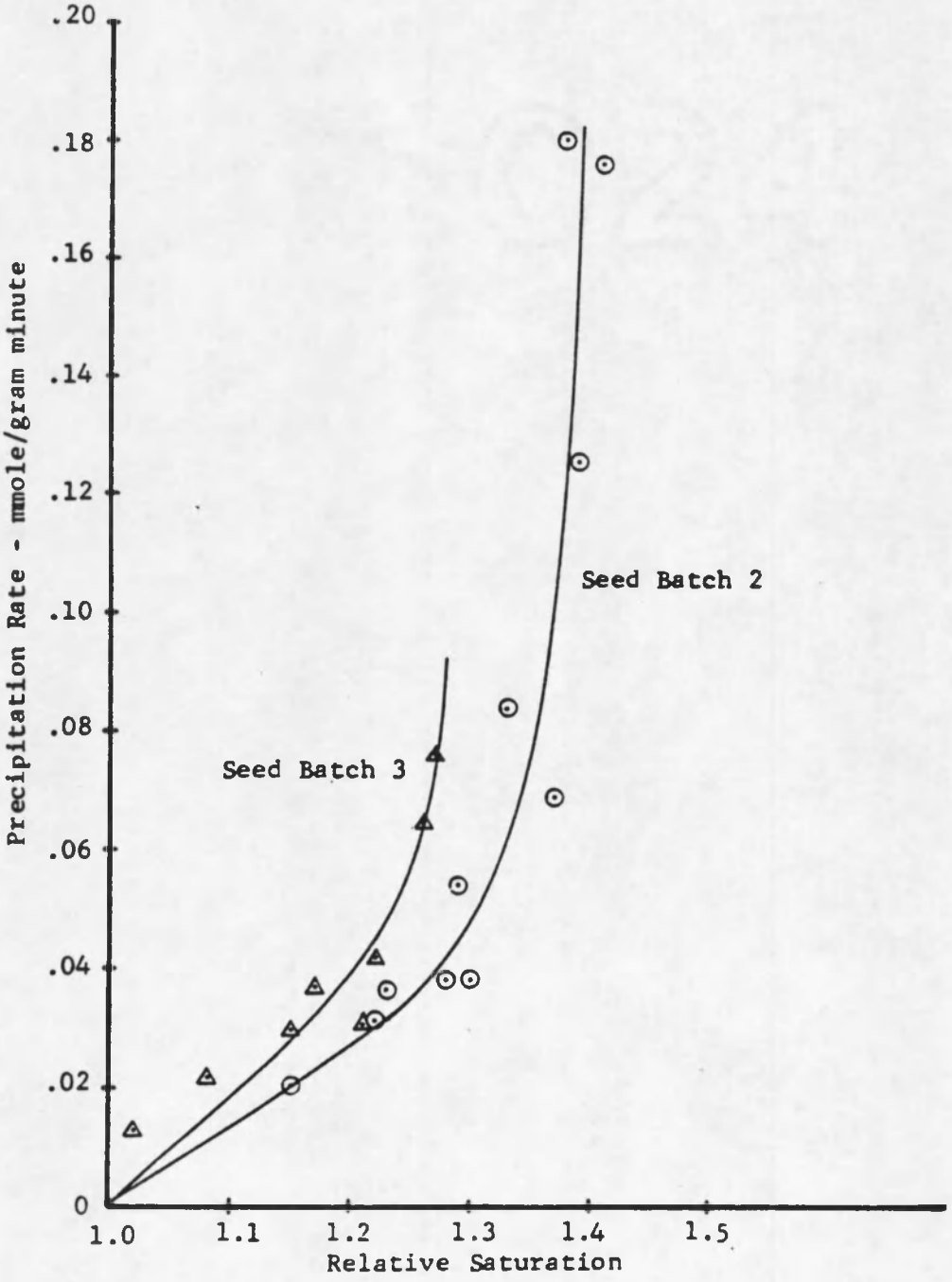

Figure 12. Precipitation Rate vs. Relative Saturation from Ottmers et al. (10).

precipitation rate to the first power of the supersaturation was proposed.

Figure 13 shows the data from the current study plotted as precipitation rate vs. supersaturation. These data show the same rapid increase in precipitation rate that Ottmers et al. (10) observed. The runs having a high nucleation rate are also shown in Figure 13. From this it can be seen that a high precipitation rate does not necessarily indicate a high nucleation rate. This indicates the importance of measuring both the growth rate and the nucleation rate.

For most runs, the increase in precipitation rate is due to increased growth as the mass of the fines distribution (i.e., precipitation on new crystals) was less than 10% of the total precipitation. In other words, the precipitation was due to growth on the seeds. The exceptions to this were the runs with both high growth and nucleation rates (i.e., runs 39, 41, and 43). In these cases, the mass of fines distribution accounted for 25-50% of the total precipitation. This also explains why no effect of stirrer rate was observed by Ottmers et al. Since RPM only affects nucleation, the change in nucleation would not be noticed when measuring precipitation.

This shows that for crystallization processes it is necessary to have information on both mass (growth) and numbers (nucleation) to adequately describe the process.

Conclusions

The growth rate is correlated with supersaturation to give a kinetic expression. High slurry densities of fine crystals can cause

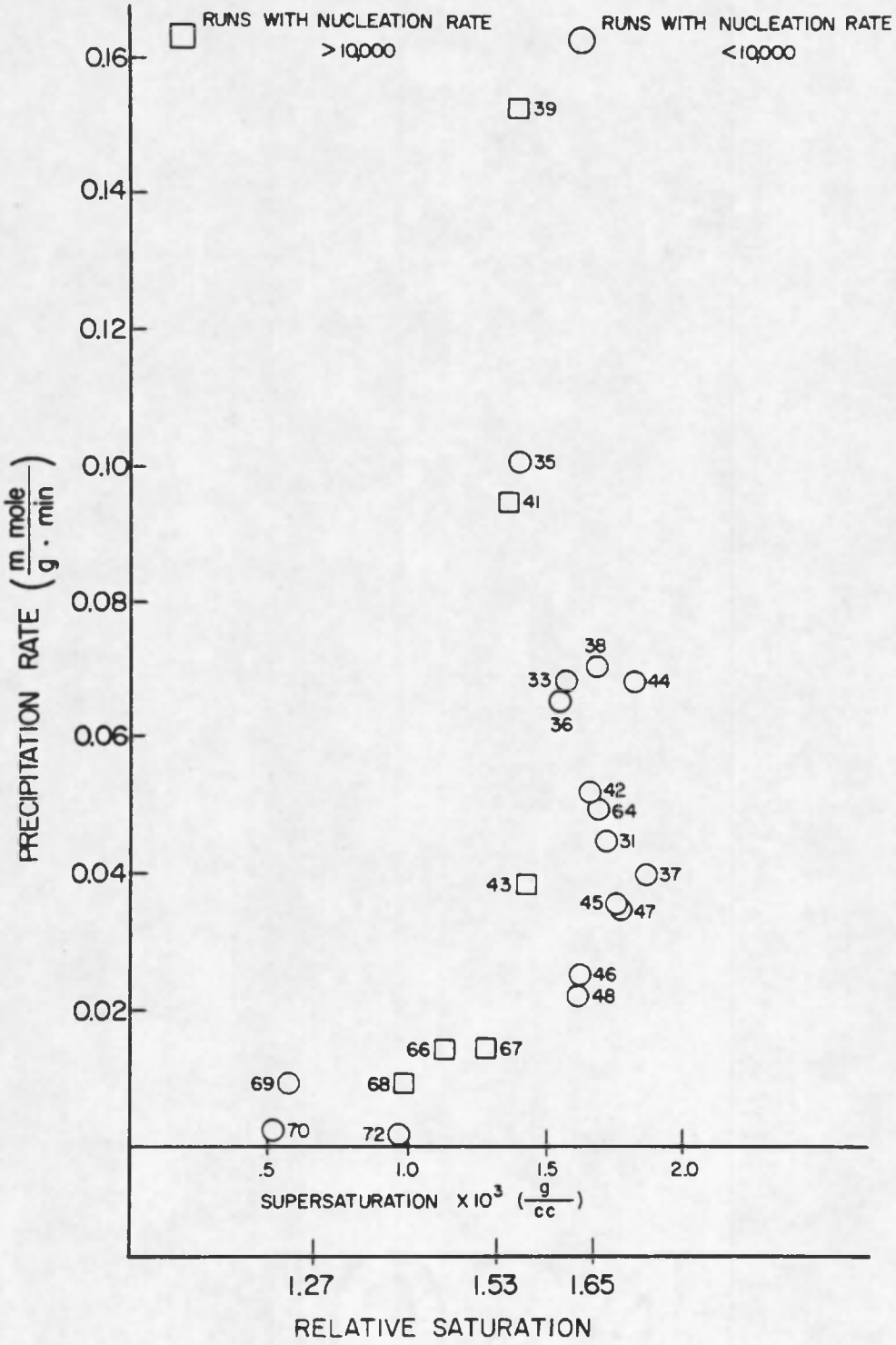

Figure 13. Data from This Study Plotted as Precipitation Rate vs. Supersaturation and Relative Saturation.

agglomeration which will increase the growth rate above the predicted by the supersaturation.

Gypsum will nucleate by either primary or secondary mechanisms depending on the conditions. If seed crystals larger than 150 microns are retained in the crystallizer and the supersaturation does not exceed the metastable limit, secondary nucleation will predominate. Since the magnitude of secondary nucleation depends on the slurry density, agitation rate and supersaturation (or growth rate), it can be correlated with these variables to give a kinetic expression that can be used to predict nucleation rates in an industrial crystallizer.

CHAPTER 6

EFFECTS OF pH LEVEL

The study of the effect of pH level on crystallization parameters is important because pH is an important design constraint affecting both solution and solid equilibria. The pH varies in different parts of a scrubber system, i.e., high pH in the tank where the lime is added and low pH in the absorber tower due to SO_2 absorption. This section briefly discusses the chemistry involved with pH changes and presents the results of this study regarding the effects of pH level on growth rate, nucleation rate, and crystal habit.

Chemistry

The normal product of the lime/limestone FGD process is calcium sulfite. In order to produce the sulfate form, oxidation must occur. The oxidation reaction that occurs in solution depends on the level of bisulfite ion as given by Equation 16:

$$HSO_3^- + \frac{1}{2} O_2 \rightleftharpoons SO_4^= + H^+ \qquad [16]$$

Since O_2 is supplied in excess, the level of bisulfite ion limits the reaction rate. Bisulfite, HSO_3^- is itself in equilibrium with $SO_3^=$ as shown in Equation 17:

$$HSO_3^- \rightleftharpoons SO_3^= + H^+ \qquad [17]$$

This equilibrium is pH dependent (Figure 14). Since HSO_3^- is the predominant product at a pH of less than 5, it is clear that low pH enhances the conversion to sulfate. pH has more effect on reaction and solution equilibris than on the solubility of calcium sulfate. A change of pH from 7.0 to 3.0 only changes the supersaturation 3%.

Procedures

pH was studied over the range 3-8. The pH of the standard make-up liquor was 7.8 and thus small amounts of H_2SO_4 were used to adjust pH to the desired level. In these runs, the pH was constant throughout a run. Crystallization parameters obtained at low pH were compared to those of normal (pH = 7.8) runs.

A second type of low pH experiment was made by adding approximately 0.1 ml H_2SO_4 to a normal run at steady state. In these runs, the pH would decrease instantaneously to about 4 or 5 and then return to 7.8 as the acid washed out. The purpose of this test was to investigate the effect of localized areas of low pH that might occur in a scrubber system as a result of poor mixing.

Observations and Results

Both growth and nucleation rates were observed to increase at low pH values. Correlating the data (see Chapter 5) as

$$B^o = k_n G^i M_T^j \qquad [18]$$

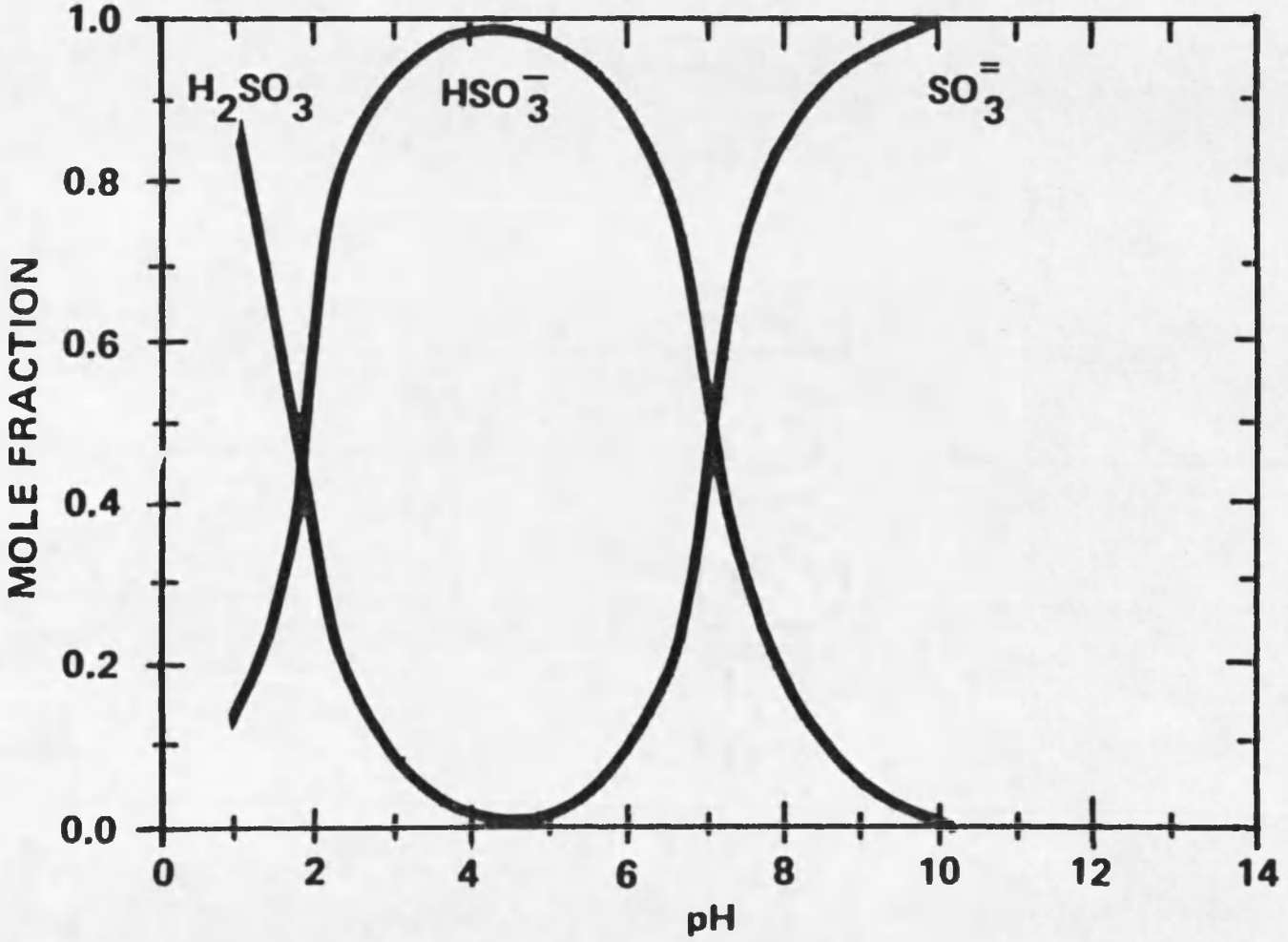

Figure 14. Sulfite-Bisulfite Equilibrium as a Function of pH.

should indicate whether or not pH should be included as another term in the correlation. The twelve data points representative of the pH range studied were correlated by the MLR routine to give:

$$B^{o} = 4473G^{1.2} M_T^{0.9} \qquad [19$$

(Note: M_T is in g/L rather than g/cc as used in Chapter 5.) The data for this correlation are plotted in Figure 15.

From Figure 15, it can be seen that there is no consistent deviation from the correlation line and that the low pH data appear to be an extension of the normal data. In other words, there is no intrinsic effect of pH other than the equilibria changes which indeed affect nucleation and growth rate in the system. pH is thus nor considered explicitly in the kinetic correlation.

In the runs where pH was instantaneously lowered, the nucleation rate was almost immediately increased and then slowly decreased back to the steady-state value as the pH returned to normal. Figure 16 shows the progression of this nucleation surge as indicated by the PDI counter.

It was also observed that when the nucleation rate was high the nuclei had a tendency to form agglomerates with each other and with the seed crystals. Agglomeration, however, was observed at both low and normal pH levels when the nucleation rate was high. Figure 17 shows some typical agglomerates.

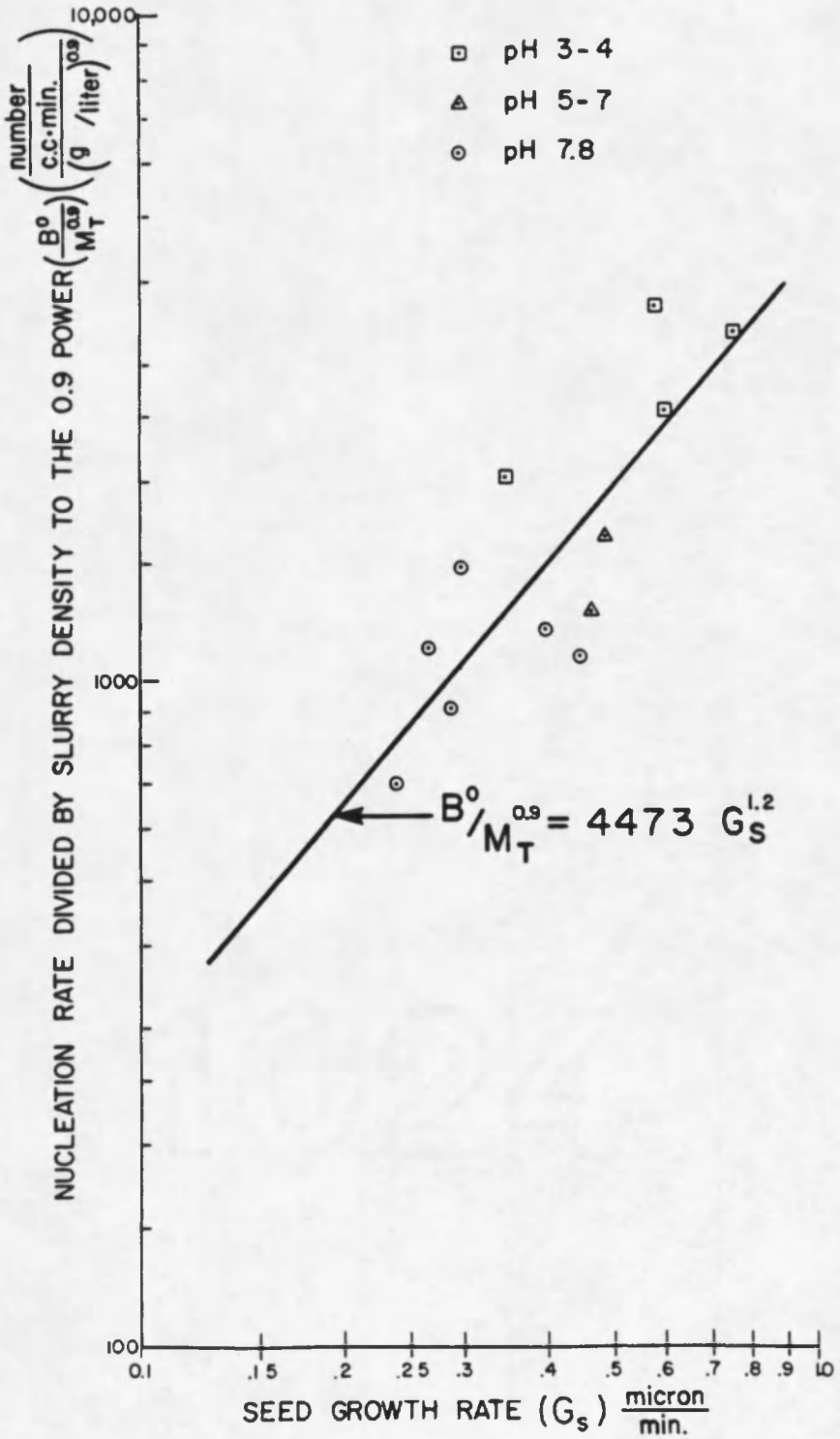

Figure 15. Correlation of Nucleation Rate at Different pH Levels.

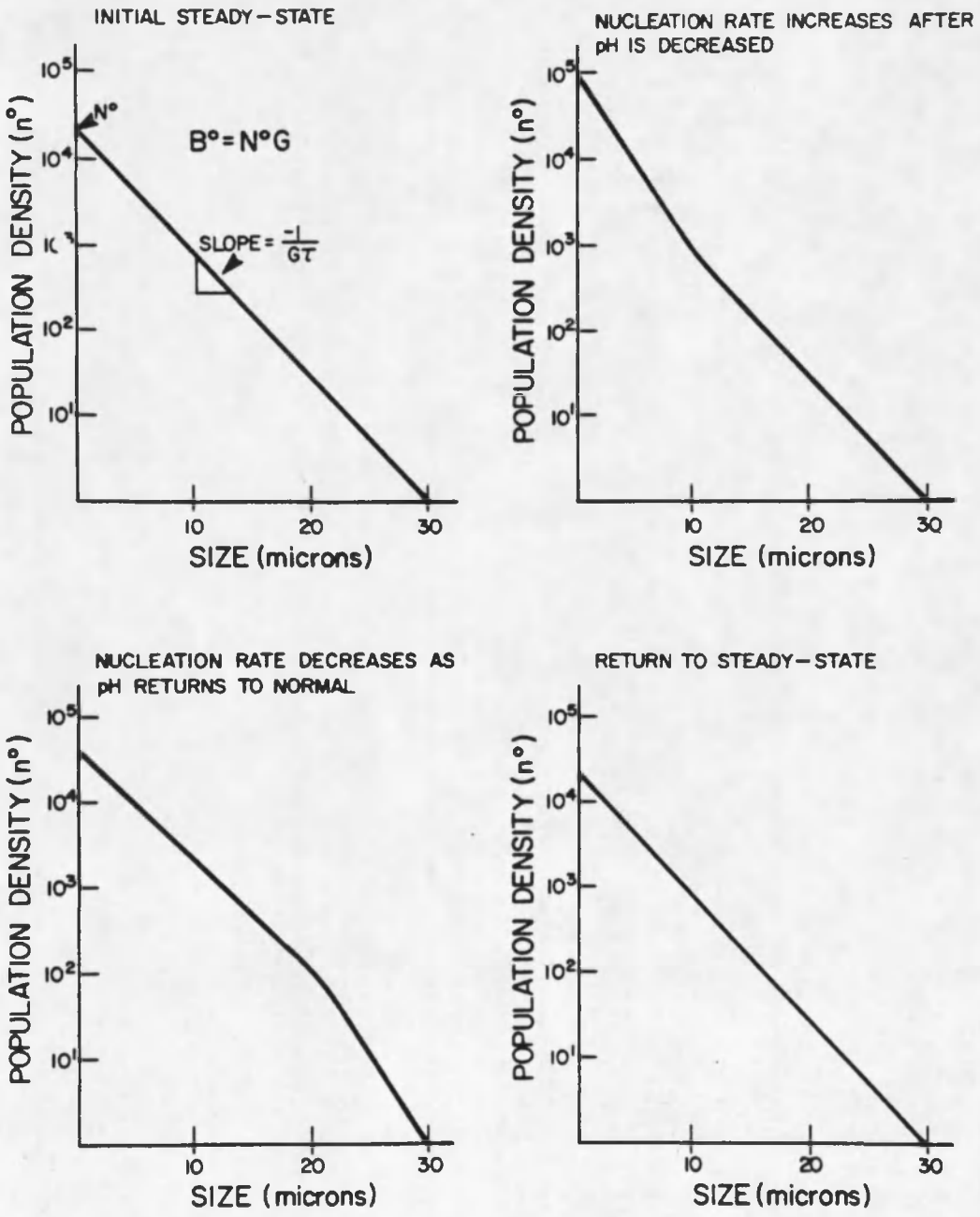

Figure 16. Progression of Nucleation Rate Surges after Low pH Pulse.

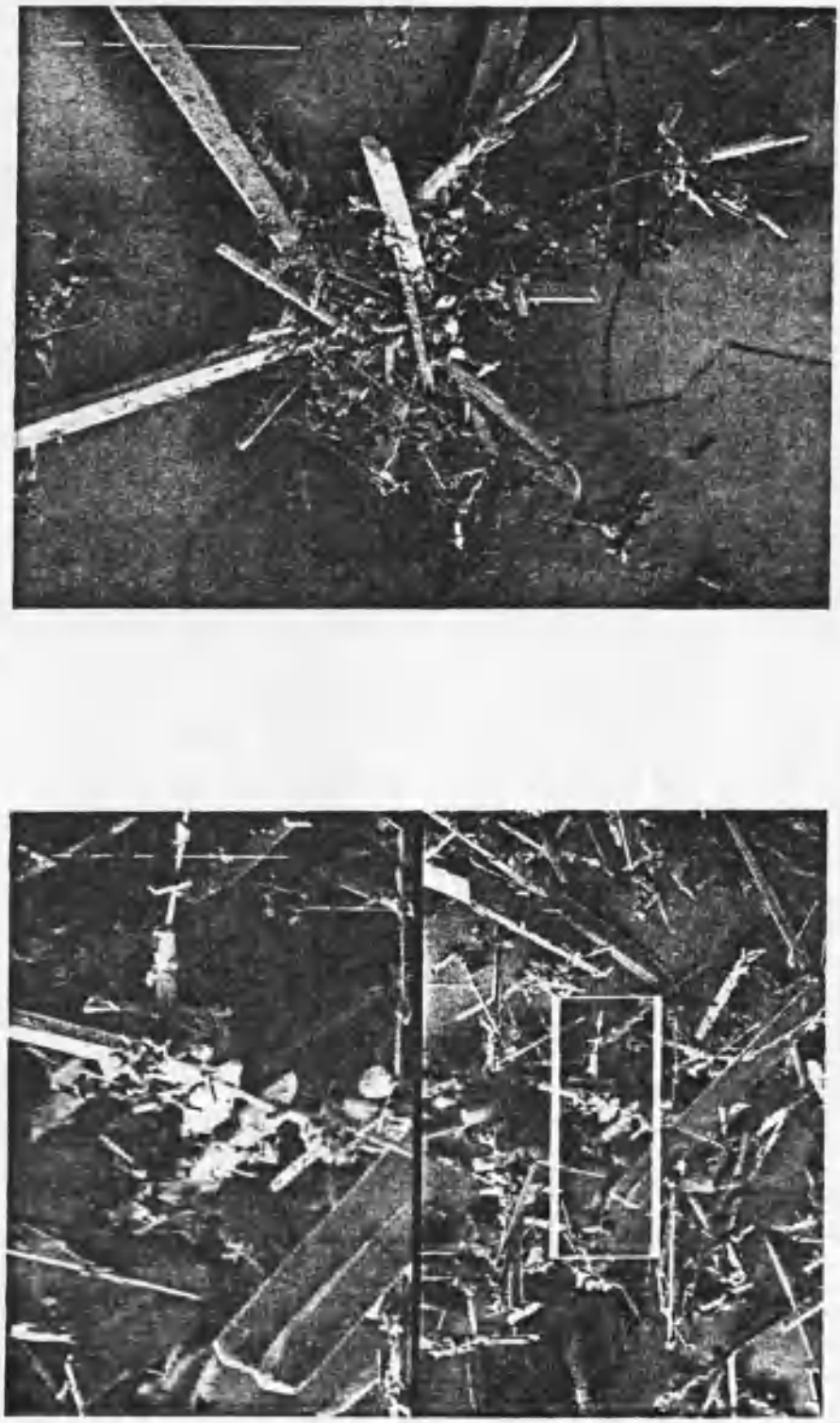

Figure 17. Typical Agglomeration of Fines.

Conclusions

Both the low pH and the pH pulse runs show that nucleation rate is increased at low pH. Low pH also causes growth rate to increase. Since the change in solubility with the pH range studied is only 3%, the increase in B^{o} and G must be explained by increased ionic activity of a rate-limiting chemical species. Whatever the reason for the increased nucleation rate at low pH, its effect on the product size is to make smaller crystals. The fact that a region of low pH will cause the nucleation to increase would also be detrimental to product size. This situation likely occurs in the poorly mixed scrubber system.

CHAPTER 7

EFFECTS OF ADDITIVES

The use of additives to modify nucleation and growth rates is a common method for improving the crystal size distribution in industrial crystallizers. Additives can also be used to change crystal habit. It is, therefore, possible that the use of additives in the crystallization of calcium sulfate sludges could produce crystals of larger size and/or better shape. This section discusses the theory and literature concerning the effects of additives and presents the results of this study for the additives sodium dodecyl benzene sulfonate (SDBS), Calgon^{R} CL246, adipic acid, and citric acid on nucleation rate, growth rate, and crystal habit.

Theory

The mechanisms by which an additive affects the properties of the crystal are tied closely to the mechanism of crystal growth. Michaels, Brian, and Beck (7) have studied the effect of SDBS on the crystallization of adipic acid and have found that growth could be both increased or decreased depending on the concentration of additive and the supersaturation. They also found that the growth rate of specific surfaces could be changed, thus altering the crystal habit. The additive is believed to adsorb on a growth site and thereby change the rate of addition of new material. The additive may also preferentially

adsorb on a particular face which would cause the growth rate to change in only one direction, thereby changing the crystal habit.

Nucleation rate can be affected by the presence of an additive by several mechanisms. If the additive modifies the growth rate and if nucleation occurs by secondary means, then the nucleation rate will be changed in accordance with the growth rate dependence of the nucleation rate correlation (discussed in Chapter 4). If the additive inhibits growth, some of the nuclei that are formed may have their growth slowed so much that they never grow to an observable size. Therefore, the apparent nucleation rate is reduced.

A different type of nucleation modification has been observed in the presence of long-chain organic acids. Sarig and Ginio (14) have shown that polyvinyl sulfonate induces heterogeneous nucleation of strontium sulfate and Thorson (16) has observed an order-of-magnitude increase in the nucleation of calcium oxalate in the presence of poly-glutamic acid. This is explained by Sarig and Ginio by proposing that the long-chain organics form microsubstrates which act as sites for heterogeneous nucleation. These polyacids have a M.W. of ~ 20,000, and therefore will be relatively motionless compared to the crystallizing molecules and thus can act as a substrate. It has been shown that in order for a particular molecule to be effective the distance between the functional groups must be close to the distance between adjacent ions in the crystal lattice.

This type of additive is used in cooling towers and heat exchangers to prevent scaling of slightly soluble salts by causing them

to precipitate in solution as fines rather than grow as a scale on the wall. It may be possible to use similar additives in stack-gas scrubbers to prevent scaling and to provide a constant level of nucleation instead of the nucleation bursts that can now occur.

McCall and Tadros (6) have studied the affect of a number of carboxylic acids on the crystal habit of calcium sulfate and calcium sulfite. They found that an "active" acid contains two or more carboxyl groups whose carbon atoms are separated by ~ 3.5 Å. This distance corresponds to the calcium-calcium distance on the {111} face of gypsum which is 3.7 Å. This suggests that the additive adsorbs on the {111} fact and lowers the growth rate, thereby causing shorter crystals. Of particular interest to this work was adipic acid, which was found to be inactive, and citric acid, which was found to alter the habit of both calcium sulfate and calcium sulfite.

Observations and Results

The additives chosen for this study have been used in stack-gas systems or have been used in other industrial environments. SDBS is a known growth modifier for other systems and therefore was studied for $CaSO_4$. Calgon^R, CL246, a mixture of poly-acrylic acids, is used as a scale preventative in cooling towers. Adipic acid is added to lime/limestone scrubbers as a pH buffer. Therefore, it is desirable to know its effect on crystallization of gypsum. Citric acid was shown to be an effective habit modifier by McCall and Tadros (6), so it seemed reasonable to confirm its effect in our system. Data for these runs are in Appendix C.

Sodium Dodecyl Benzene Sulfonate

Past studies have shown SDBS to be effective at the ppm level and therefore it was used at 10-40 ppm in this study. SDBS was obtained from the Continental Oil Company (company name: Conoco C560) as 40% SDBS in alcohol.

SDBS shows no effect (or a slight reduction) in nucleation and growth rates at 9 ppm compared to a blank run. At 35 and 40 ppm, however, growth rate is reduced and nucleation rate is increased. The results of run #50 show that if SDBS is added after a normal steady state is reached, fines growth rate decreases and the nucleation rate increases. The difference in seed growth cannot be determined, since the seed growth rate is only determined at the end of the run, and is an average growth rate with and without SDBS. There was no difference in crystal habit using SDBS.

Calgon^{R} CL246

This additive was added to the crystallizer during several runs after the no-additive steady state was reached. The additive concentration was 100 to 500 ppm. Immediately after addition, high levels of nucleation were observed. Crystal habit was not changed except for the agglomeration that normally occurred at high nucleation rates.

Adipic Acid

Adipic acid was used at concentrations of 1.0 to 6.0 g/L. The pH for these runs was about 3.0. Nucleation rate for these runs was generally higher than for normal runs and lower than for no-additive,

low pH runs. The growth rates were similar to all other runs. As expected, the crystal habit was not affected by the presence of adipic acid.

Citric Acid

Citric acid was used only at a concentration of 1.0 g/L. The supersaturation had to be raised in order for nucleation to occur. Growth rates were much lower than predicted from the normal correlation assuming the calculated value of supersaturation remained valid. Figure 18 shows growth rate vs. supersaturation for the citric acid runs compared to the correlation obtained with no additives. This increase in the apparent supersaturation was also observed by McCall and Tadros (6). The use of citric acid in the absorber liquor in the citrate/ Citrex^{R} process (4) increases the amount of SO_2 absorbed by a factor of fifty. This increased solubility is probably due to changes in solution equilibrium which are not accounted for in the equilibrium program. Thus, calculated values of supersaturation used in Figure 18 are probably in error when citric acid is used as an additive.

The nuculeation rate behavior was similar to that obtained with adipic acid, but the crystal habit was changed markedly (Figure 19). The results of this study are in agreement with data of McCall and Tadros (6) showing decreased growth on the {111} face which resulted in blockier crystals.

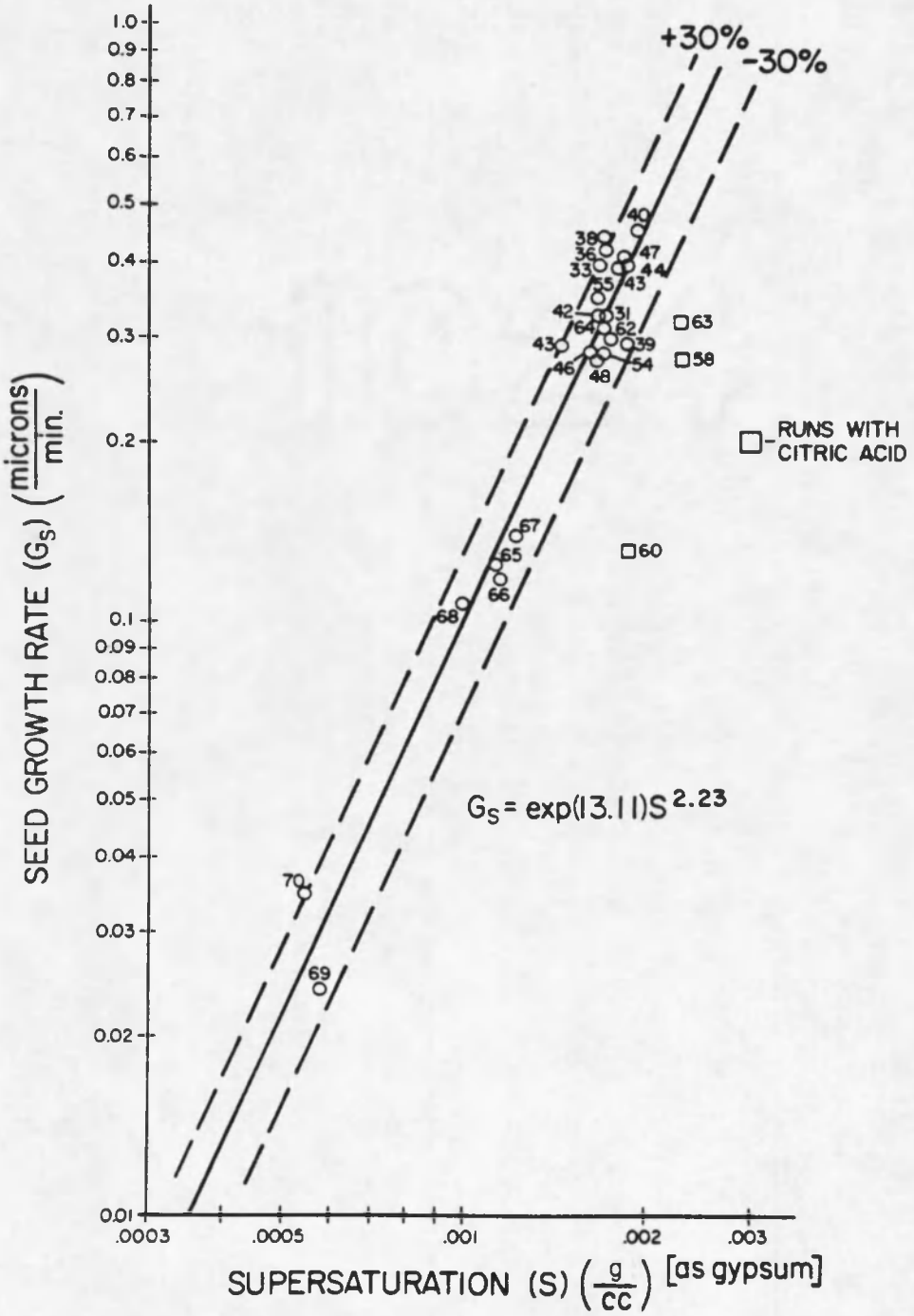

Figure 18. Deviation from Growth Correlation with Use of Citric Acid.

a)

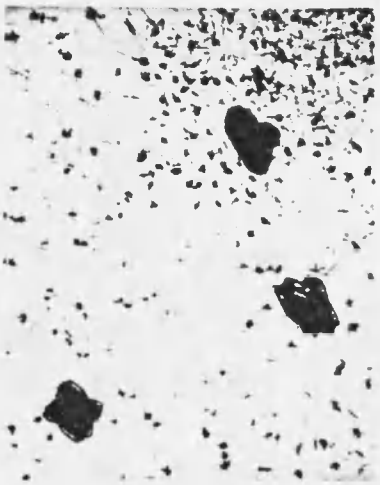

b)

c)

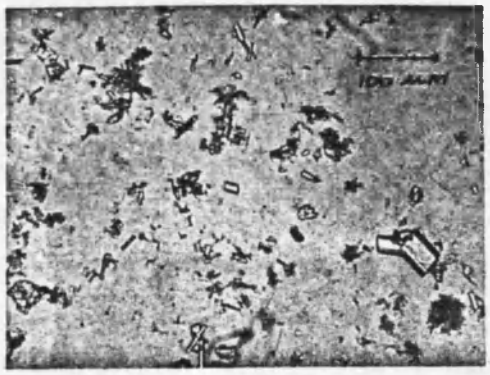

Figure 19. Fine Crystals: a) Normal Agglomerates; b) Needle-Like Crystals; and c) Crystals Grown in the Presence of Citric Acid.

Conclusions

Desirable effects of an additive would be to decrease the ratio of nucleation to growth rates and to change the crystal habit from needles to blockier crystals. Adipic acid is neutral in this respect. Since most sulfate systems are operated at a pH of 5.0-6.0, the nucleation/growth rate ratio with adipic acid would be about the same as without any additive. Since crystal habit is also not changed, adipic acid has no effect from a crystallization point of view. Its use as a pH buffer in scrubber liquor is not detrimental to crystallization, but is also not beneficial. SDBS and CL246 are detrimental since they increase nucleation and give either a decrease or no effect on growth rate. They may be helpful, however, since they cause nucleation at a constant level rather than the surges that can occur. The quantitative effects of high nucleation rates are discussed in Chapter 8.

Further study of the effect of citric acid on gypsum crystallization appears to be warranted, especially at lower concentrations (< 1 g/L). Lower concentrations should have less of a solubilizing effect on gypsum. Certainly the growth of gypsum with a blockier habit could result in significantly better dewatering.

CHAPTER 8

CSD MODELING

The growth and nucleation kinetics presented in Chapter 5 can be used in conjunction with mass and population balances and given design parameters (e.g., vessel volume, feed supersaturation, liquid and solid residence times) to predict the crystal size distribution of the calcium sulfate product from a scrubber precipitator. A computer simulation program (Mark I CSD Simulator) has been developed previously (9) at The University of Arizona to predict CSD from various crystallizer designs. Mark I was used to study the effects on CSD of varying the liquid vs. solid residence times and high levels of nucleation which might be caused by localized low pH and/or additives which enhance heterogeneous nucleation.

Simulation Procedures

The Mark I simulator simultaneously solves population and mass balances, growth kinetics, and nucleation kinetics to give the steady-state CSD of the crystallizer product. This program can simulate single- or multi-stage crystallizers with or without product classification and fines destruction. Mark I was used to simulate a single-stage gypsum crystallizer with and without classified product removal.

Classified product removal (in this case retention of larger-sized product) is accomplished by installing some type of classification

device to the exit stream. One stream of the classification device is returned to the crystallizer and the other is removed. The result of such classification would be to cause the crystals to have a size-dependent residence time. Proper selection of the size-dependence would produce larger crystals. Classification in the case studied can be achieved simply by the installation of an internal vessel baffle, thus permitting removal of a partially clarified overflow together with a mixed heavy-slurry underflow. Both underflow and overflow streams would be fed to the existing clarifier (see Figure 22, Proposed Design, page 61).

The TVA Shawnee test facility production rates and vessel sizes were used as the basis for the model. Figure 20a is a schematic of a scrubber. Due to the high recycle ratio, the scrubber and hold tank can be considered as one vessel for crystallization purposes, and therefore the system reduces to Figure 20b for modeling purposes. The volume of the crystallizer is taken as 20,000 gallons. From the withdrawal rate of 25 gpm and a production of 6 tons/day of gypsum, an apparent feed relief of supersaturation of 0.04 g/cc is calculated. This value represents the concentration of gypsum that must precipitate to satisfy the mass balance. The computer simulation will calculate the actual supersaturation present in the scrubber as well as the CSD using the nucleation/growth rate kinetics supplied to the program.

In order to model a scrubber, it is necessary to know the size of the particles that are returned to the crystallizer in the clarifier overflow stream. A sample of the Shawnee clarifier overflow was

a)

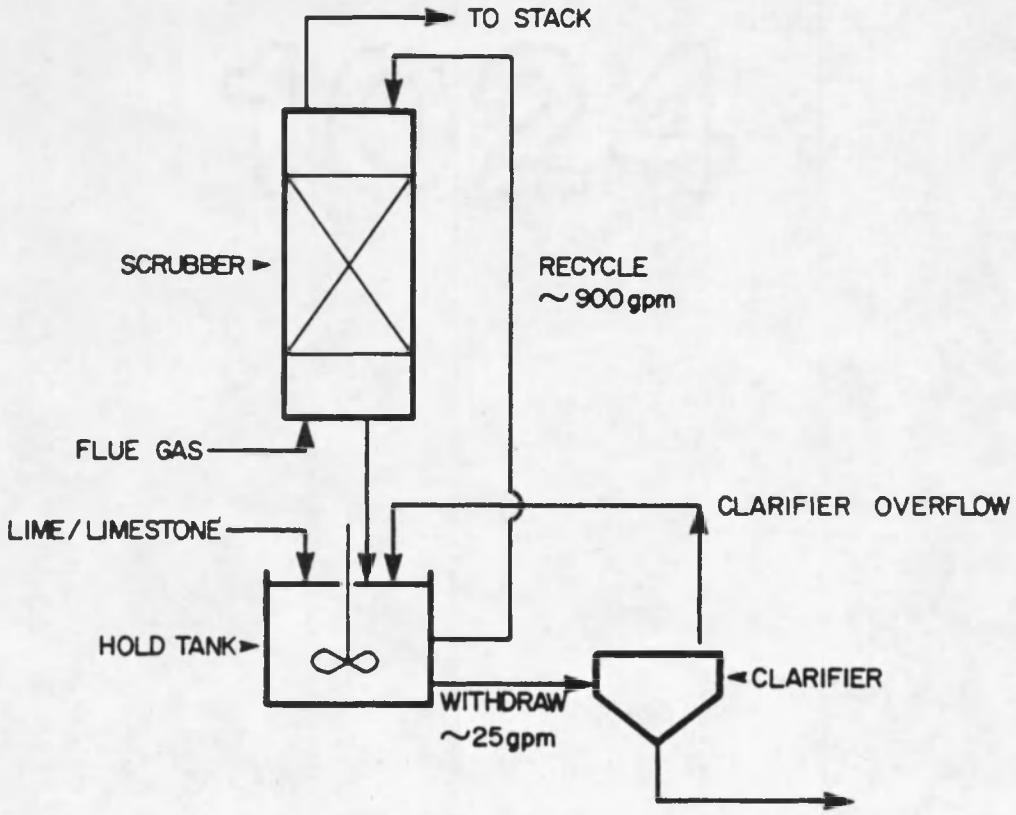

b)

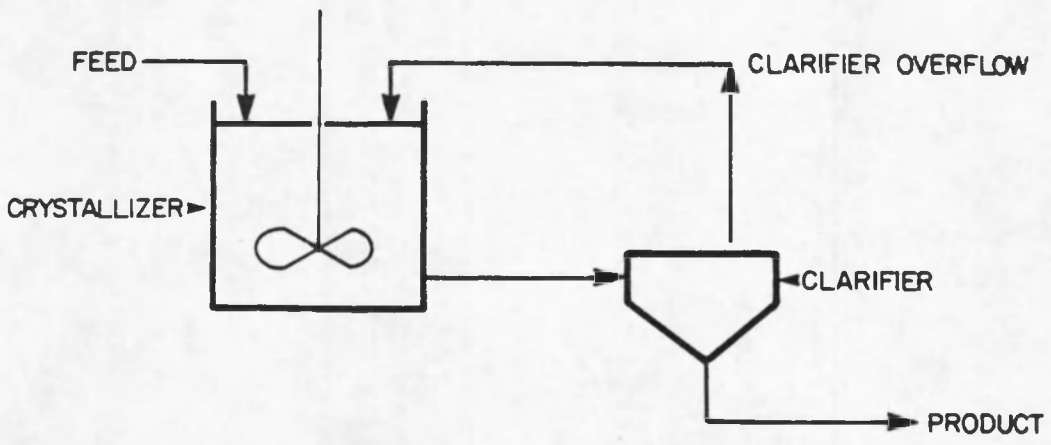

Figure 20. Scrubber Configurations: a) Actual Configuration; b) Configuration Used for Modeling Purposes.

obtained and the size distribution was determined with the PDI counter. From Figure 21 it can be seen that most of the particles are below 10-15 microns, therefore 15 microns will be used as the classification size of the clarifier.

Three configurations with different liquid-solid residence times were modeled. They were mixed suspension mixed product removal (MSMPR), the current configuration of the Shawnee facility, and the proposed design. Figure 22 shows the schematic of each configuration and the form of the classification function, which is the ratio of the flow rate of particles in a given size range to the flow rate in the mixed removal stream.

The MSMPR configuration is considered to be the base case with no classification. That is, the liquid and solid residence times are equal, therefore the classification function is constant for all sizes. The current Shawnee design operates with classified removal since the fine particles in the clarifier overflow are returned to the crystallizer. Therefore, crystals smaller than 15 microns are removed at a lower rate than those in a mixed suspension. The proposed design would incorporate a baffle-type settler inside the crystallizer. This baffle would provide a zone of low mixing where large particles would settle back into the mixing zone and small particles would be removed. The small particles would be removed at an accelerated rate compared to the mixed suspension. However, the clarifier overflow would still return particles less than 15 microns to the crystallizer (as this is a design constraint on the clarifier) and thus they would be removed at a lower

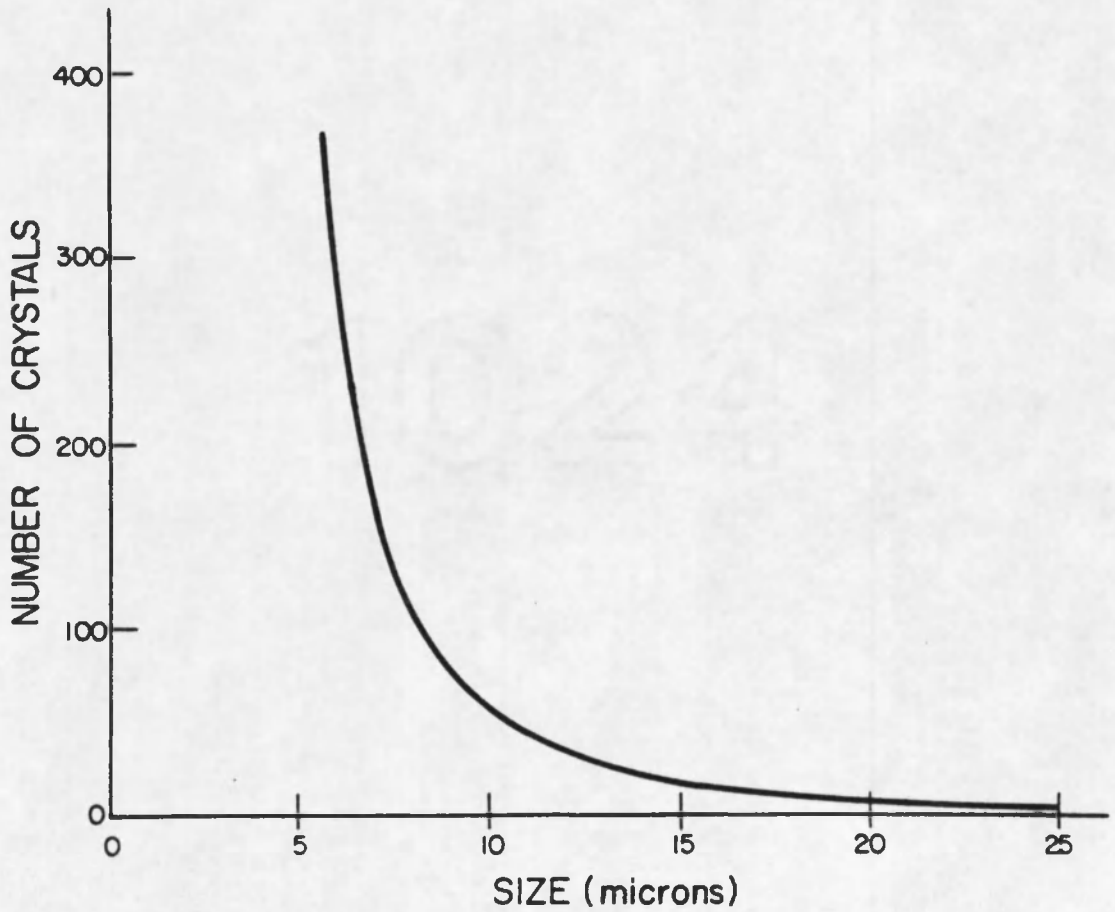

Figure 21. Size Distribution of the Clarifier Overflow Stream.

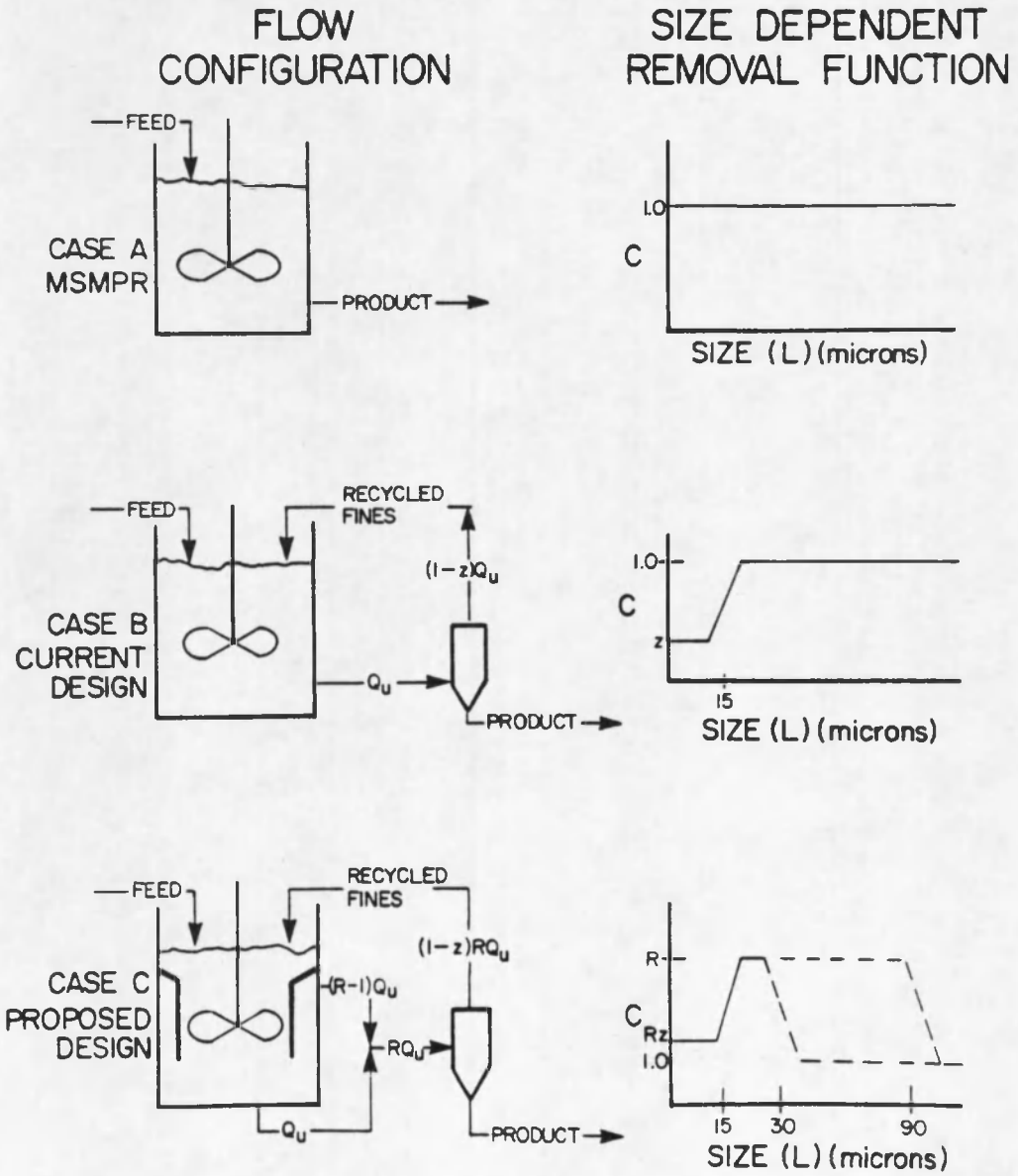

Figure 22. Configurations Simulated in This Study.

rate than particles between 15 microns and the upper classification size. The upper classification size and the removal ratios are variables which depend on particle hydraulics and settler design. Classification sizes of 30-70 microns and removal ratios of 3 to 10 were simulated in order to determine the conditions giving the best size improvement.

The effects of high nucleation rates were simulated by replacing the kinetic expression with a constant value of nucleation. This simulates the constant nucleation rate that might be produced by certain additives and gives the upper asymptotic limit of nucleation caused by localized zones of low pH as measured in this study of gypsum kinetics.

Results and Discussion

The calculated product sizes resulting from the three configurations simulated are as follows:

Configuration	Mean Size (Mass Weighted Basis) (microns)
MSMPR	71
Current design	67
Proposed design	83-130

These results show that returning the clarifier overflow to the crystallizer has a detrimental effect on the crystal size compared to the MSMPR case. The proposed design, which preferentially retains larger crystals, would result in an improvement in crystal size.

Figure 23 shows the size of the crystals in the crystallizer (b) and in the product (a) as a function of the classification size and the removal ratio. The product size increases with increasing fines removal ratio and decreasing classification size to 50 microns, then levels off or decreases. The size of particles in the crystallizer also increases with increasing removal ratio, but reaches a maximum as a function of classification size. The classification size at which the maximum occurs increases with increasing removal ratio.

From Figure 23 it appears that a good design would be a classification size of 50 microns and a removal ratio of 7. This design gives a product size of 117 microns and a size in the crystallizer of 180 microns. Thus, the product size has increased by a factor of two over the current design. Such classified retention should be readily achievable in the gypsum-water system.

In order to study the effect of high nucleation rate, the kinetic expression for nucleation rate was replaced by a constant value. This was done for the MSMPR, the current design, and the optimum proposed design cases using nucleation rates of 4,000, 8,000, and 20,000 number/cc·min). The product size for each of these cases is given in Table 3. The nucleation rate calculated using the experimental correlation was between 1,000 and 2,500 for these three cases.

Increasing the nucleation rate causes significant reduction of product size in all cases and, in fact, ultimately invalidates the benefits of the proposed design. Nucleation rates of 4,000 to 8,000 would be expected in areas of localized low pH. The average nucleation rate

a)

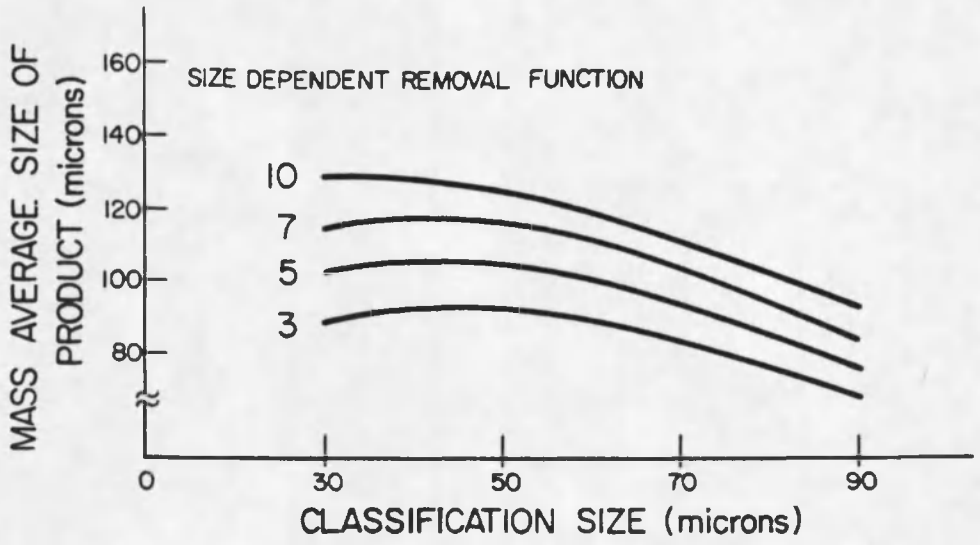

b)

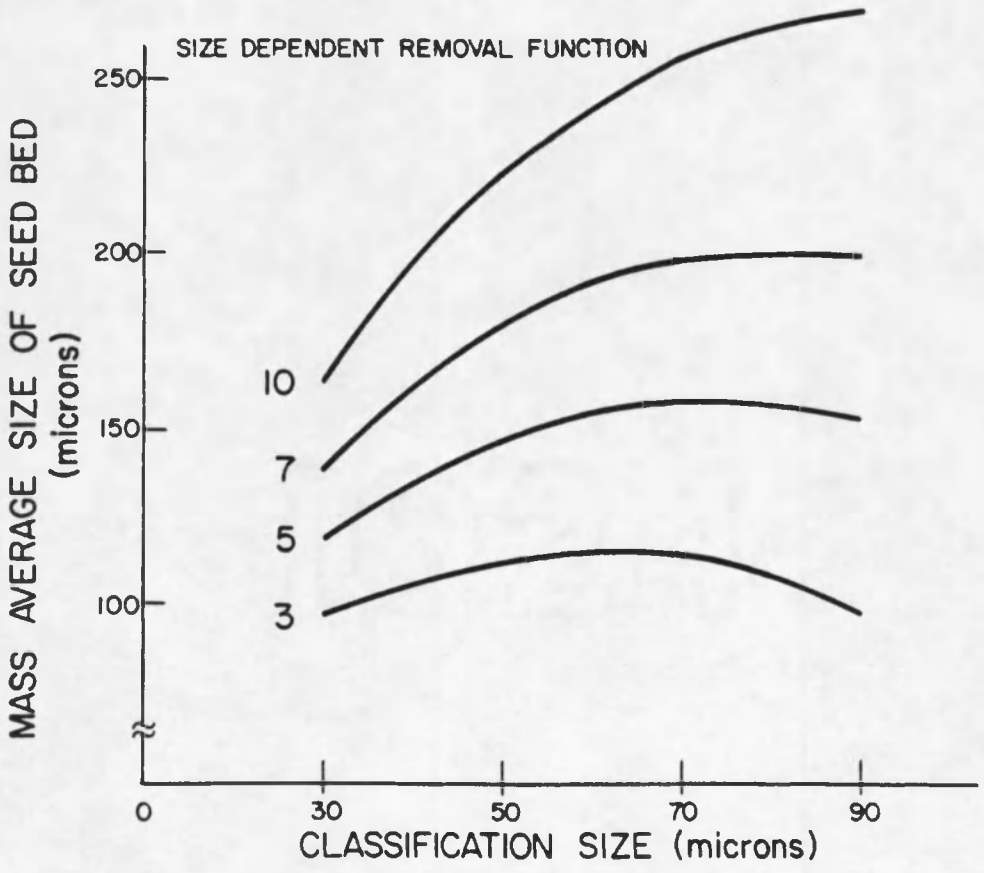

Figure 23. Mass Average Size of Product (a) and Retained Seeds (b), as a Function of Classification Size and Removal Ratio.

Table 3. Results of High Nucleation Rate Simulation.

Nucleation Rate	MSMPR (microns)	Current Design (microns)	Proposed Optimum Design (microns)
Experimental kinetics expression	71	67	117
4,000	48	39.8	77
8,000	38	30.4	29.7
20,000	28	21.6	16.1

and therefore particle size would be somewhere between the values given by the experimental kinetics and the high nucleation rates. Nucleation rates of 8,000 to 20,000 occur in the presence of heterogeneous nucleation enhancers. It is desirable to eliminate both of these sources of nuclei if the particle size is to be maximized.

These results also show that the proposed design, utiliting accelerated fines removal, is even more sensitive to increased nucleation rates than the MSMPR or the current design. This can be explained by recalling that particles less than the classification size are removed at an accelerated rate. Therefore, when the average particle size approaches or falls below the classification size the effect is to remove the product faster than the fines. In other words, there is an accelerated removal of the largest crystals in the distribution resulting in a finer product size and the classification range is

ill-chosen. The solution to this problem of course is to reduce the classification size or, better still, to maintain low nucleation rates.

Because of the increased particle size and the accelerated removal of fines, the area of crystals in the crystallizer will be reduced. This could cause increased fouling on the scrubber intervals, as fouling is known to occur if sufficient crystal area is not provided in the scrubber. The crystal area is dependent on the classification size and the removal ratio just as is the product size. Therefore, some trade-offs may be required between increased particle size and increased tendency to foul.

Conclusions

A crystallizer design that will accelerate the removal of small crystals relative to larger ones should produce a larger particle size. This type of crystallizer is common in industry and the resulting size improvement over the MSMPR crystallizer is well-known. The key to successful operation of this type of crystallizer is the ability to control, or at least to predict, the nucleation rate. This is best done by operating under conditions where secondary nucleation is the predominate source of nuclei. Crystallization modeling should be combined with scrubber operating experience to provide an integrated design of the proposed precipitator configuration.

CHAPTER 9

CONCLUSIONS

1. Nucleation and growth rates of calcium sulfate dihydrate (gypsum) crystals were measured in simulated stack-gas liquors as a function of supersaturation, pH, slurry density, agitation rate, and chemical additives. These data were correlated to give design-useful kinetic expressions. The effect of additives on crystal habit was also observed.
2. From the study of the effects of supersaturation, slurry density and agitation rate, it was shown that gypsum nucleates by secondary nucleation mechanisms when crystals greater than 150 microns are retained in the slurry. However, bursts of primary nucleation, which decreases particle size, will occur if the supersaturation becomes too high or if seed crystals are not present.
3. Low pH was found to increase both growth and nucleation rates. Regions of low pH (or sudden decreases in pH) produced bursts of nucleation resulting in smaller crystals.
4. Additives studied were sodium dodecyl benzene sulfonate, polyacrylates, adipic acid, and citric acid. Of these, only citric acid improved the crystal habit by producing blockier crystals rather than the needle-like crystals normally produced.

5. The kinetic expressions obtained in this study were used in a computer simulation model to predict the product size for various crystallizer configurations. Particle size could be nearly doubled by using a double-drawoff configuration where the fine crystals are removed at an accelerated rate as compared to the mixed removal. This type of operation is attained by installing an internal settling baffle in the crystallizer.

APPENDIX A

GROWTH RATE AND SUPERSATURATION DATA

Run No.	Initial Seed Mass (g)	Initial Seed Size (micron)	Final Seed Mass (g)	Final Seed Size (micron)	Run Time (min)	Growth Rate (micron/min)	Mass Gain (g)	Production (g/L)	Equilibrium Solids as Given by Equilibrium Program (g/L)	Actual Supersaturation $(S)x10^3$ (g/cc)
31	2.00	193	6.60	287	285	0.330	4.60	0.323	2.05	1.73
33	2.00	193	6.45	285	227	0.408	4.45	0.392	2.05	1.66
32	1.00	193	2.08	246	208	0.255	1.08	0.104	--	--
35	2.00	193	7.01	293	176	0.568	5.01	0.569	2.13	1.56
36	2.00	193	7.08	294	237	0.427	5.08	0.429	2.13	1.70
37	2.00	193	5.12	280	295	0.296	4.12	0.279	2.13	1.85
38	2.00	193	7.59	301	240	0.450	5.59	0.349	2.05	1.70
39	2.00	193	5.39	268	135	0.560	3.39	0.376	2.19	1.81
40	2.00	193	4.74	257	138	0.466	2.74	0.199	2.13	1.93
41	2.00	193	11.16	342	288	0.518	9.16	0.477	1.95	1.47
42	2.00	193	8.38	311	355	0.333	6.38	0.269	1.95	1.68
43	5.00	193	13.44	268	255	0.295	8.44	0.496	1.95	1.45
44	2.00	193	9.74	327	330	0.400	7.74	0.352	2.19	1.84
45	2.00	273	4.73	364	225	0.403	2.73	0.182	1.95	1.77
46	5.00	273	10.58	350	270	0.287	5.58	0.310	1.95	1.64
47	2.00	273	4.37	354	195	0.417	2.37	0.182	1.95	1.84
48	5.00	273	9.38	337	230	0.277	4.38	0.286	1.95	1.66
49	2.00	185	2.20	191	180	0.033	0.20	0.017	1.95	1.93
50	2.00	185	5.13	253	300	0.230	3.13	0.156	1.95	1.79
51	2.00	185	6.30	271	300	0.290	4.30	0.215	1.95	1.74
52	2.00	185	2.50	200	180	0.083	0.50	0.042	--	--
53	2.00	185	6.21	270	150	0.566	4.21	0.421	1.88	1.46
54	2.00	185	5.09	253	240	0.282	3.09	0.193	1.89	1.70
55	2.00	185	6.23	270	240	0.355	4.23	0.264	1.91	1.65
56	2.00	185	5.65	261	160	0.478	3.65	0.342	1.84	1.50

Run No.	Initial Seed Mass (g)	Initial Seed Size (micron)	Final Seed Mass (g)	Final Seed Size (micron)	Run Time (min)	Growth Rate (micron/min)	Mass Gain (g)	Production (g/L)	Equilibrium Solids as Given by Equilibrium Program (g/L)	Actual Supersaturation $(S)x10^3$ (g/cc)
57	2.00	185	2.16	--	--	--	0.16	--	1.95	1.91
58	2.00	185	6.78	278	330	0.281	4.78	0.217	2.51	2.29
59	2.00	185	2.12	189	240	0.017	0.12	0.007	1.95	1.94
60	2.00	185	3.33	219	255	0.133	1.33	0.078	1.95	1.87
61	2.00	185	4.93	250	300	0.216	2.93	0.148	1.95	1.80
62	2.00	185	5.69	262	255	0.302	3.69	0.217	1.95	1.73
63	2.00	185	5.42	258	225	0.324	3.42	0.228	2.51	2.28
64	2.00	185	7.30	285	315	0.317	5.30	0.252	1.95	1.70
65	2.00	185	4.88	249	510	0.125	2.88	0.085	1.22	1.135
66	21.8	185	41.05	228	360	0.119	19.25	0.802	1.95	1.15
67	20.0	229	37.6	280	360	0.140	17.6	0.733	1.95	1.22
68	20.0	229	32.7	270	375	0.109	12.7	0.508	1.505	0.997
69	20.0	273	22.0	282	375	0.024	2.0	0.080	0.66	0.580
70	20.0	273	21.4	279	180	0.035	1.4	0.117	0.66	0.543
71	20.0	273	24.1	290	200	0.088	4.1	0.307	0.90	0.683
72	20.0	273	21.0	277	240	0.019	1.0	0.062	0.99	0.928
73	20.0	277	23.8	289	180	0.066	3.8	0.230	1.32	1.09

APPENDIX B

DATA FOR NUCLEATION RATE CORRELATION

Run No.	Growth Rate (G_s) (micron/min)	Slurry Density (M_T) [g/cc ($x10^3$)]	Nucleation Rate (B^o) (number/cc·min)	Comments
31	0.330	4.61	6,400	
32	0.255	1.87	4,000	
33	0.406	5.24	7,500	
35	0.568	5.22	5,000	
36	0.427	6.20	6,500	
37	0.296	5.29	4,500	
38	0.450	5.18	5,500	
39	0.560	4.01/5.14	10,000/12,000	
40	0.466	4.12	10,000	
41	0.518	10.02	14,000	
42	0.333	6.60/8.12	4,000/4,500	
43	0.295	12.15	11,000	
44	0.406	9.21	5,900	
45	0.403	3.85	3,400	
46	0.287	10.20	5,300	
47	0.417	4.03	3,600	
48	0.277	9.15	5,100	
49	0.033	2.20	--	Runs with SDBS
50	0.230	5.00	--	
51	0.290	6.30	3,300	
52	0.083	2.45	--	
53	0.566	5.64	7,000	
54	0.282	4.84	3,500	
55	0.355	5.75	8,000	
56	0.478	5.35	8,700	
57	0.011	2.16	0	
58	0.281	5.89	8,700	
59	0.017	2.00	0	

Run No.	Growth Rate (G_s) (micron/min)	Slurry Density (M_T) [g/cc ($x10^3$)]	Nucleation Rate (B^o) (number/cc·min)	Comments
60	0.133	3.33	--	
61	0.216	3.25	3,000	
62	0.302	5.12	7,500	Run with Shawnee liquor
63	0.324	5.22	6,900	
64	0.317	6.59	10,000	
65	0.125	4.33	0	
66	0.119	41.00	10,000	
67	0.140	28.7/37.6	12,000/30,000	
68	0.109	32.00	18,000	
69	0.024	22.00	500	
70	0.035	21.40	1,000	
71	0.088	24.10	--	
72	0.019	21.00	300	
73	0.066	23.80	--	Run with Shawnee liquor

APPENDIX C

DATA FOR RUNS WITH ADDITIVES

Run No.	Additive	Concentration of Additive	Supersaturation [(g/cc) x10^3]	Growth Rate (G_s) (micron/min)	Slurry Density (M_T)x10^3 (g/cc)	Nucleation Rate (B^o) (number/cc·min)	Comments
49	SDBS	42 ppm	1.93	0.033	2.20	60,000	
50		35 ppm	1.79	0.230	5.00	40,000	
51		9 ppm	1.74	0.290	6.30	3,300	
52		20 ppm	1.51	0.083	2.45	0	
26	Calgon	200 ppm	1.81	--	--	bursts	Additive added to steady-state run
29	CL246	500 ppm	1.76	--	--	bursts	
53	Adipic	4.0 g/L	1.46	0.566	5.64	7,000	
54	acid	2.0 g/L	1.70	0.282	4.84	3,500	
55		1.0 g/L	1.65	0.355	5.75	8,000	
56		6.0 g/L	1.50	0.478	5.35	8,700	
65		5.0 g/L	1.13	0.125	4.33	0	
57	Citric	1.0 g/L	1.91	0.011	2.16	0	
58	acid	1.0 g/L	2.29	0.281	5.89	8,700	
59		1.0 g/L	1.94	0.017	2.00	0	
60		1.0 g/L	1.87	0.133	3.33	3,000	
63		1.0 g/L	2.28	0.324	5.22	6,900	

LIST OF REFERENCES

1. Burton, W. K., N. Cabrera, and F. C. Frank, Phil. Trans. Roy. Soc., London, A243, 299 (1951).

2. Cise, M. D., Crystal Growth and Nucleation Kinetics of the Potassium Sulfate System in a Continuous-Flow Crystallizer, Ph.D. Dissertation, University of Arizona, Tucson (1971).

3. Clontz, N. A., and W. L. McCabe, CEP Symp. Series, 67(110), 6 (1971).

4. Chereminsinoff, P. N., and R. A. Young (eds.), Air Pollution Control and Design Handbook Part 2, Marcel Dekker, Inc., New York, p. 891 (1977).

5. Larson, M. A., D. C. Timm, and P. R. Wolff, AIChE J., 14, 448 (1968).

6. McCall, T., and M. E. Tadros, Effects of Additives on Morphology of Precipitated Calcium Sulfate and Calcium Sulfite -- Implications on Slurry Properties, unpublished manuscript, Martin Marietta Corp., Baltimore (1979).

7. Michaels, A. S., P. L. T. Brian, and W. F. Beck, Cinemicrographic Studies of Single Crystal Growth: Effects of Surface Active Agents on Adipic Acid Crystals Grown from Aqueous Solution, AIChE 57th Annual Meeting (1964).

8. Murray, D. C., and M. A. Larson, AIChE J., 11, 728 (1965).

9. Nuttall, H. E., Computer Simulation of Steady State and Dynamic Crystallizers, Ph.D. Dissertation, University of Arizona, Tucson (1971).

10. Ottmers, D., Jr., J. Phillips, C. Burklin, W. Corbett, N. Phillips, and C. Shelton, A Theoretical and Experimental Study of the Lime/Limestone Wet Scrubbing Process, EPA-650/2-75-006 (1974).

11. Randolph, A. D., and M. A. Larson, AIChE J., 8(5), 639 (1962).

12. Randolph, A. D., and M. A. Larson, Theory of Particular Process, Academic Press, New York (1971).

13. Randolph, A. D., and K. Rajagopal, I&EC Fund., 9, 165 (1970).

14. Sarig, S., and O. Ginio, A Mechanism for Retarded Precipitation Based on the Time Evolution of Particle Size and Relative Number Density, J. Phy. Chem., 80(3), 256 (1976).

15. Timm, D. C., and T. R. Cooper, AIChE J., 17, 285 (1971).

16. Thorson, S, A Study of Calcium Oxalate Dihydrate Crystallization in Synthetic and Human Urines, M.S. Thesis, University of Arizona, Tucson (1979).

4175. 4